Calhoun: The NPS Institutional Archive

DSpace Repository

Theses and Dissertations | 1. Thesis and Dissertation Collection, all items

1992-03

Method of moments analysis of displaced-axis dual reflector antennas

Vered, Nissan

Monterey, California. Naval Postgraduate School

http://hdl.handle.net/10945/38558

Copyright is reserved by the copyright owner.

Downloaded from NPS Archive: Calhoun

http://www.nps.edu/library

Calhoun is the Naval Postgraduate School's public access digital repository for research materials and institutional publications created by the NPS community. Calhoun is named for Professor of Mathematics Guy K. Calhoun, NPS's first appointed -- and published -- scholarly author.

Dudley Knox Library / Naval Postgraduate School
411 Dyer Road / 1 University Circle
Monterey, California USA 93943

AD-A247 970

NAVAL POSTGRADUATE SCHOOL
Monterey, California

DTIC
ELECTE
MAR 26 1992
S B D

THESIS

METHOD OF MOMENTS ANALYSIS OF
DISPLACED-AXIS DUAL
REFLECTOR ANTENNAS

by

Nissan Vered

March 1992

Thesis Advisor: David C. Jenn

Approved for public release; distribution is unlimited

92-07631

REPORT DOCUMENTATION PAGE

UNCLASSIFIED	
	Approved for public release; distribution is unlimited
Naval Postgraduate School (EC)	Naval Postgraduate School
Monterey, CA 93943-5000	Monterey, CA 93943-5000

METHOD OF MOMENTS ANALYSIS OF DISPLACED-AXIS DUAL REFLECTOR ANTENNAS

VERED, Nissan

Master's Thesis		March 1992	79

The views expressed in this thesis are those of the author and do not reflect the official policy or position of the Department of Defense or the US Government.

	method of moments analysis of displaced-axis dual reflector antennas

Small symmetric dual reflector antennas suffer from low efficiency due to subreflector blockage of the main reflector and subreflector scattering. These can be reduced by slicing the main dish and translating its rotational axis, along with modifying of the subreflector geometry.

This type of design is usually applied to low-frequency reflectors, but high-frequency analysis techniques are used. Consequently the agreement between measured and computer data is not as good as it would be for a rigorous solution such as the method of moments.

This thesis modifies an existing method of moments computer code to handle the displaced axis geometry, and computes the radiation pattern and the efficiency of this antenna as a function of geometrical and electrical design parameters. Optimum configurations are identified for several feed types.

X	UNCLASSIFIED
JENN, David C.	408-646-2254 EC/Jn

DD Form 1473, JUN 86

Approved for public release; distribution is unlimited.

METHOD OF MOMENTS ANALYSIS OF DISPLACED-AXIS DUAL REFLECTOR ANTENNAS

by

Nissan Vered
Lieutenant Commander, Israeli Navy
B.S.C., Israel, Haifa, Technion, 1987

Submitted in partial fulfillment
of the requirements for the degree of

MASTER OF SCIENCE IN ELECTRICAL ENGINEERING

from the

NAVAL POSTGRADUATE SCHOOL
March 1992

Author: [redacted]

Nissan Vered

Approved by: [redacted]

David C. Jenn, Thesis Advisor

[redacted]

H. M. Lee, Second Reader

[redacted]

Michael A. Morgan, Chairman,
Department of Electrical and Computer Engineering

ABSTRACT

Small symmetric dual reflector antennas suffer from low efficiency due to subreflector blockage of the main reflector and subreflector scattering. These can be reduced by slicing the main dish and translating its rotational axis, along with modifying the subreflector geometry.

This type of design is usually applied to low-frequency reflectors, but high-frequency analysis techniques are used. Consequently the agreement between measured and computed data is not as good as it would be for a rigorous solution such as the method of moments.

This thesis modifies an existing method of moments computer code to handle the displaced axis geometry, and computes the radiation pattern and the efficiency of this antenna as a function of geometrical and electrical design parameters. Optimum configurations are identified for several feed types.

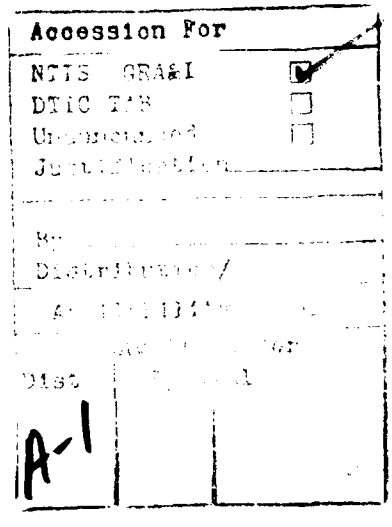

TABLE OF CONTENTS

I. INTRODUCTION 1

A. DUAL-REFLECTOR ANTENNA SYSTEMS 1

B. DISPLACED AXIS DUAL-REFLECTOR ANTENNA SYSTEMS . 4

C. SCOPE OF THE STUDY 6

II. INTEGRAL EQUATIONS AND THE MOMENT METHOD 7

A. ELECTRIC FIELD INTEGRAL EQUATION 7

B. SOLUTION OF THE EFIE USING THE METHOD OF MOMENTS 9

C. MM SOLUTION FOR THE SPECIAL CASE OF BODIES OF REVOLUTION 12

D. MEASUREMENT MATRICES 15

III. METHOD OF MOMENTS SOLUTION FOR ADE ANTENNA . . . 17

A. CALCULATION OF IMPEDANCE ELEMENTS 17

B. EVALUATION OF THE EXCITATION VECTOR 29

IV. COMPUTER PROGRAM 32

A. THE MAIN PROGRAM 32

1. The ADE Antenna Radiation Patterr 32

2. Gain Program 35

B. THE SUBROUTINE SPHERE 35

C. THE SUBROUTINE ZMAT 36

D. THE SUBROUTINES DECOMP AND SOLVE 36

E. THE SUBROUTINES PLANE AND PLAN 37

V. COMPUTED RESULTS 38

VI. SUMMARY AND CONCLUSIONS 45

APPENDIX 47

LIST OF REFERENCES 71

INITIAL DISTRIBUTION LIST 72

ACKNOWLEDGEMENT

This thesis is the summary of research efforts over the last year and reflects part of the knowledge and skills that were passed to me during my study in the Electrical Engineering Department of the Naval Postgraduate School. I would like to thank my wife, Irit, for her support and understanding, the members of the academic staff who contributed their time and effort to my education, foremost of them my advisor Professor David C. Jenn.

I. INTRODUCTION

A. DUAL-REFLECTOR ANTENNA SYSTEMS

The paraboloidal antenna with a feed at the focus does not allow much control of the power distribution over the aperture surface, except for what can be accomplished by changing the focal length and feed pattern. The introduction of a second reflecting surface, such as in the Cassegrain or Gregorian systems, allows more control of the aperture distribution because of the extra degree of freedom that a second reflecting surface gives. This additional control over the aperture field distribution is obtained by shaping both the subreflector and the main reflector so as to change the power distribution on the main reflector aperture but yet maintain the required phase distribution. A single reflector does not allow both the power and phase distribution to be varied independently [Ref. 1].

In general these types of antennas provide a variety of benefits, such as the

- ability to place the feed in a convenient location
- reduction of spillover and minor lobe radiation
- ability to obtain an equivalent focal length much greater than the physical length
- capability for scanning and/or broadening of the beam

by moving one of the reflecting surfaces [Ref. 2].

The Cassegrain antenna, which is shown in Figure 1 and derived from telescope design [Ref. 3], is the most common antenna using multiple reflectors. The feed illuminates the hyperboloidal subreflector, which in turn illuminates the paraboloidal main reflector. The feed is placed at one focus of the hyperboloid and the paraboloid focus at the other. A similar system is the Gregorian, which uses an ellipsoidal subreflector in place of the hyperboloid as shown in Figure 2.

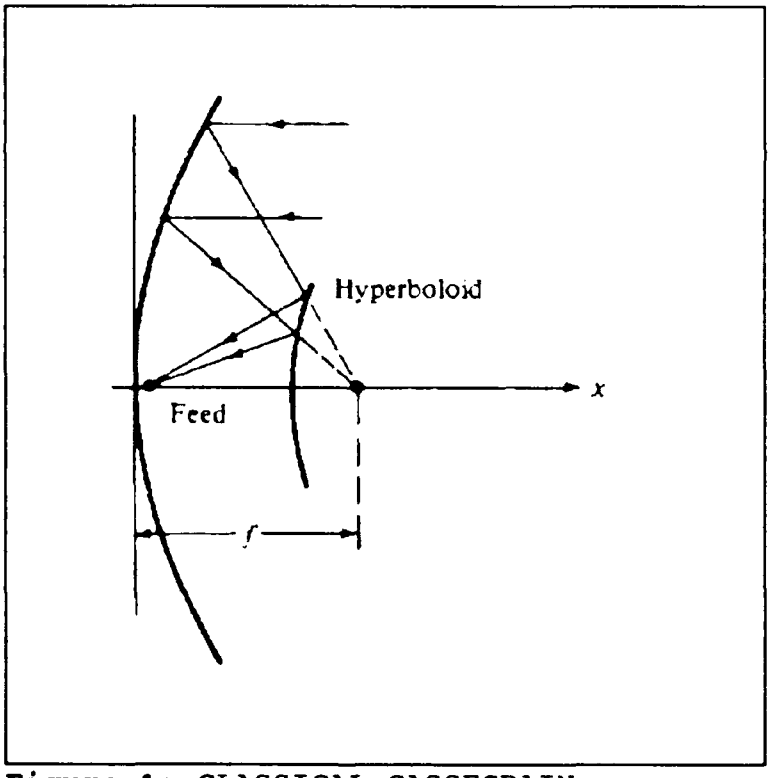

Figure 1: CLASSICAL CASSEGRAIN

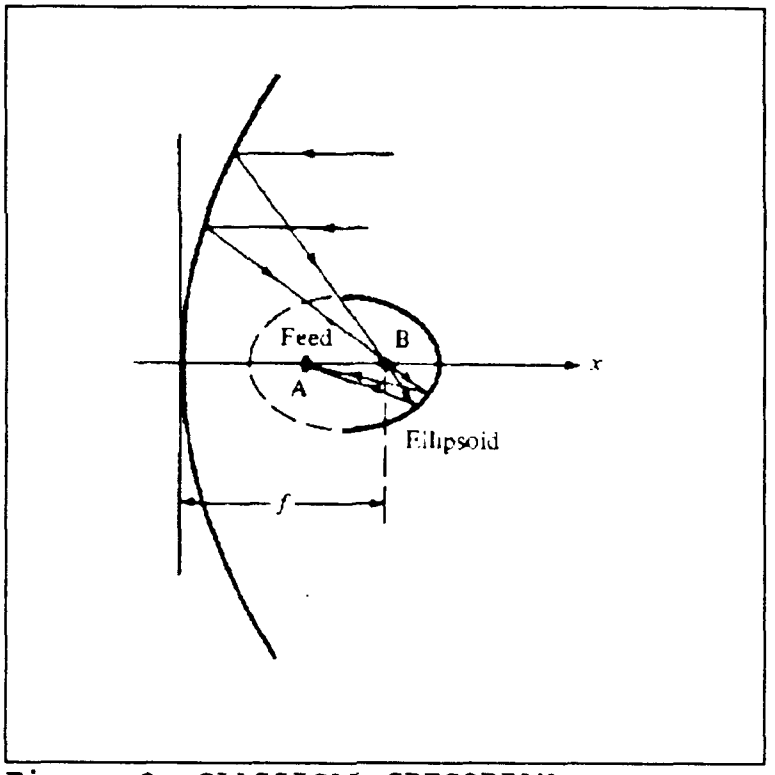

Figure 2: CLASSICAL GREGORIAN

Aperture blocking can be large for these types of antennas. It may be minimized by choosing the diameter of the subreflector equal to that of the feed. This "minimum blocking condition" is derived using geometrical optics and does not always give good results for electrically small antennas.

In the general dual-reflector case, blockage can be eliminated by either of two ways:

(1) offsetting both the feed and the subreflector [Ref. 4] and

(2) displacing the main reflector and compensating for the displacement by reorienting the subreflector.

In the latter case rotational symmetry is maintained.

B. DISPLACED AXIS DUAL-REFLECTOR ANTENNA SYSTEMS

Mobile satellite communication terminals require **small antennas with high aperture efficiencies**. The Cassegrain and Gregorian antenna types, which are simple and therefore inexpensive, are generally not suitable for this purpose since their subreflectors have a relatively large blocking area, causing a reduction in gain. In other words, they have low efficiency for the sizes of interest (20 to 30 wavelengths).

One method of reducing blockage, yet maintaining rotational symmetry, is to displace the main reflector away from the axis of symmetry and then adjust the subreflector so that a plane wave front is achieved in the aperture plane. A displaced-axis antenna with a subreflector that is a portion of a hyperboloid will be called an **ATH** for short, and one with elliptical based subreflector an **ATE** (or **ADE**). Geometrical optics analysis of the ATE and ATH can be found in [Ref. 5].

As mentioned earlier, the ADE antenna may be considered as a special case of the generalized Gregorian system. However in this case the focal axis of the main parabolic reflector is displaced from the axis of symmetry, which contains the prime focus of the elliptical subreflector as shown in Figure 3. The locus of the secondary foci of the subreflector forms a ring through which all the rays pass, which coincides with the ring focus of the main reflector. The parameters of the ellipse and the parabola are chosen so that the central ray from the prime focus reaches the outer edge of the main

reflector, while the inner ray clears the outer edge of the subreflector after reflection from the main reflector.

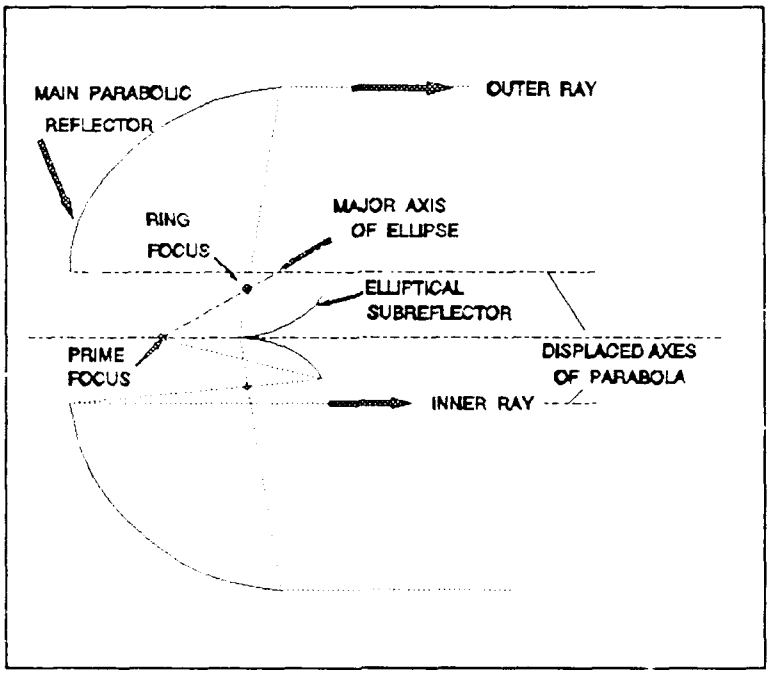

Figure 3: DISPLACED AXIS ANTENNA (ADE)

The principal merits of this geometry are that the rays are not reflected into the prime feed from the subreflector, nor back into the subreflector from the main reflector. Also, the aperture illumination for the radiated wave is more uniform than that in the standard Cassegrain or Gregorian configuration. All rays reflected from the paraboloid miss the subreflector, leading to a higher aperture efficiency. Another advantage of the ADE antenna is that the F/D ratio of the main reflector can be made smaller than that for a regular design, leading to a compact antenna design with a reduction in far-out sidelobes [Ref. 6].

To summarize, the advantages of this type of design are

- the main reflector may be made as small as ten wavelengths while retaining a relatively high efficiency
- a low feed input reflection coefficient can be achieved
- small sidelobe and gain degradation due to aperture blockage
- elimination of the spares which normally hold the subreflector (the subreflector can usually be integrated into the feed design for small antennas).
- subreflectors which can be several times smaller than those in Cassegrain antennas.

C. SCOPE OF THE STUDY

Chapter II discusses the derivation and the **MM** solution of the electric field integral equation for a general body of revolution (**BOR**) and measurements matrices are developed. Chapter III discusses the **MM** solution for the **ADE** antenna geometry and evaluates the excitation vector for an ideal feed. Chapter IV explains the computer program that has been developed based on an existing code written by Mautz and Harrington. Chapter V discusses the results obtained by the program and presents some guidelines for optimizing the geometry. Chapter VI discusses conclusions based on the results and presents some recommendations for further research.

II. INTEGRAL EQUATIONS AND THE MOMENT METHOD

A. ELECTRIC FIELD INTEGRAL EQUATION

In the following analysis time-harmonic field quantities are assumed. Phasor representations of the fields are used with the $e^{j\omega t}$ time dependence suppressed.

The electric field integral equation (EFIE) is based on the boundary condition that the total tangential electric field on a perfectly electric conducting (PEC) surface of an antenna or scatterer is zero. Then the total field **E** is the sum of the incident and scattered fields. This can be expressed as

$$\boldsymbol{E}^{t}_{\tan} = \boldsymbol{E}^{i}_{\tan} + \boldsymbol{E}^{s}_{\tan} = 0 \quad on\ S \tag{1}$$

where **S** is the conducting surface of the antenna or scatterer. The subscript 'tan' indicates tangential components. The incident field that impinges on the surface S induces an electric current density $\mathbf{J}_s$, which in turn radiates the scattered field.

The scattered field can be expressed in terms of a vector potential **A** and a scalar potential **Φ** as

$$\boldsymbol{E}^{s}(\boldsymbol{r}) = -j\omega\boldsymbol{A} - \nabla\Phi \tag{2}$$

where

$$\boldsymbol{A} = \mu \iint_{s} \boldsymbol{J}_s \frac{e^{-jkR}}{4\pi R}\, ds' \tag{3}$$

$$\mathbf{R} = |\mathbf{r} - \mathbf{r}'| \tag{4}$$

where $\mathbf{r}'$ is the point source location, and $\mathbf{r}$ is the observation point location and

$$\Phi = \frac{1}{\epsilon}\iint_s \rho_s \frac{e^{-jkR}}{4\pi R}\, ds' \ . \tag{5}$$

The continuity equation relates the current and charge on the surface

$$\nabla\cdot\boldsymbol{J}_s = -j\omega\rho_s \tag{6}$$

or

$$\Phi = \frac{j}{\omega\mu\epsilon}\nabla\cdot\mathbf{A} \ . \tag{7}$$

Substitution of (3) and (7) into (2) gives the following equation

$$\boldsymbol{E}^s(\boldsymbol{r}) = j\omega\mu\iint_s \boldsymbol{J}_s(\boldsymbol{r}')\,\frac{e^{-jkR}}{4\pi R}\,ds' + \frac{j}{\omega\epsilon}\nabla[\nabla\cdot\iint_s \boldsymbol{J}_s(\boldsymbol{r}')\,\frac{e^{-jkR}}{4\pi R}\,ds'] \ . \tag{8}$$

This is the most general form of the EFIE. Let the free space Green's function be denoted as

$$G(\boldsymbol{r},\boldsymbol{r}') = \frac{e^{-jkR}}{4\pi R} = \frac{e^{-jk|\boldsymbol{r}-\boldsymbol{r}'|}}{4\pi|\boldsymbol{r}-\boldsymbol{r}'|} \tag{9}$$

so that (8) becomes

$$\boldsymbol{E}^s(\boldsymbol{r}) = j\omega\mu\iint_s \boldsymbol{J}_s(\boldsymbol{r}')\,G(\boldsymbol{r},\boldsymbol{r}')\,ds' + \frac{j}{\omega\epsilon}\nabla[\nabla\cdot\iint_s \boldsymbol{J}_s(\boldsymbol{r}')\,G(\boldsymbol{r},\boldsymbol{r}')\,ds' \ . \tag{10}$$

$\mathbf{J}_s$ only depends on the primed quantities and G is a scalar that depends on both the primed and unprimed quantities. $\mathbf{J}_s$ is the unknown quantity to be solved for.

For convinience, define an operator $\mathcal{L}$ which operates on J_s

$$\mathcal{L}(\boldsymbol{J}_s) = j\omega\mu \iint_s \boldsymbol{J}_s(\boldsymbol{r}')\, G(\boldsymbol{r},\boldsymbol{r}')\, ds' + \frac{j}{\omega\epsilon} \nabla \left[\nabla \cdot \iint_s \boldsymbol{J}_s(\boldsymbol{r}')\, G(\boldsymbol{r},\boldsymbol{r}')\, ds'\right] . \tag{11}$$

After using vector identities and modifying the last term

$$\mathcal{L}(\boldsymbol{J}_s) = j\omega\mu \iint_s \boldsymbol{J}_s(\boldsymbol{r}')\, G(\boldsymbol{r},\boldsymbol{r}')\, ds' + \nabla \left[\iint_s \nabla G(\boldsymbol{r},\boldsymbol{r}') \cdot \boldsymbol{J}_s(\boldsymbol{r}')\, ds'\right] . \tag{12}$$

Since $\nabla G = -\nabla' G$, where ∇' is defined with respect to the source quantities,

$$\iint_s \nabla G(\boldsymbol{r},\boldsymbol{r}') \cdot \boldsymbol{J}_s(\boldsymbol{r}')\, ds' = -\iint_s \nabla' G(\boldsymbol{r},\boldsymbol{r}') \cdot \boldsymbol{J}_s(\boldsymbol{r}')\, ds' . \tag{13}$$

Using vector identities and the surface divergence theorem, it can be shown that

$$\mathcal{L}(\boldsymbol{J}_s) = \iint_s \left[j\omega\mu\, \boldsymbol{J}_s(\boldsymbol{r}')\, G(\boldsymbol{r},\boldsymbol{r}') - \frac{j}{\omega\epsilon} \nabla \left[(\nabla' \cdot \boldsymbol{J}_s(\boldsymbol{r}')\,)\, G(\boldsymbol{r},\boldsymbol{r}') \right] \right] ds' . \tag{14}$$

The EFIE can now be written consisely as

$$\mathcal{L}(\boldsymbol{J}_s) = \boldsymbol{E}^i_{\tan} . \tag{15}$$

More detail on the development of the EFIE is available in [Ref. 7] and in [Ref. 8].

B. SOLUTION OF THE EFIE USING THE METHOD OF MOMENTS

To solve (15) the method of moments is used. The method of moments generates a generalized impedance matrix for the body of interest. The excitation of the body is represented by a voltage matrix, and the resultant current on the body is

represented by a current matrix [Ref. 2]. Equation (15) is reduced to a matrix equation, which can then be solved using standard methods.

The analysis and solution presented here are for the special case of bodies which are rotationally symmetric about an axis. Because of this symmetry a Fourier series expansion in the angle of rotational symmetry reduces the problem to a system of independent modes. This is important from the view of computation; several small matrices must be inverted instead of one large one.

The first step in the MM procedure is to expand $\mathbf{J}_s$ into a series

$$\boldsymbol{J}_s = \sum_{j=1}^{N} I_j \boldsymbol{J}_j \qquad (16)$$

where I_j are the expansion coefficients to be determined and the $\mathbf{J}_j$ are called basis or expansion functions.

The $\mathbf{J}_j$ are usually chosen to be:

(1) consistent with the behavior of the actual current on the surface,

(2) mathematically convenient (i.e. have certain desirable mathematical properties which will be discussed later).

Equation (16) is substituted into (15), which, because of the linearity of $\mathcal{L}$, becomes

$$\sum_j I_j \mathcal{L}(\boldsymbol{J}_j) = \boldsymbol{E}^i_{\tan} \qquad (17)$$

Similarity a set of N testing function $\{\mathbf{W}_i\}$ is defined. Although they need not be related to the set of basis functions, they are usually chosen to be their complex conjugate (Galerkin's Method). Now the inner product is defined

$$\langle \boldsymbol{W}, \boldsymbol{J} \rangle = \iint_s \boldsymbol{W} \cdot \boldsymbol{J} ds \qquad (18)$$

where **W** and **J** are tangential vectors on S. Taking the inner product of both sides of the EFIE (equation (17))

$$\sum_j I_j \langle \boldsymbol{W}_i, \mathfrak{L}(\boldsymbol{J}_j) \rangle = \langle \boldsymbol{W}_i, \boldsymbol{E}^i \rangle \quad i = 1, 2, 3, \ldots, N . \qquad (19)$$

The subscript 'tan' has been dropped from $\mathbf{E}^i$ because the inner product involves only tangential components. Now define

$$\boldsymbol{V}_i = \langle \boldsymbol{W}_i, \boldsymbol{E}^i \rangle \qquad (20)$$

$$\mathbf{Z}_{ij} = \langle \mathbf{W}_i, \mathfrak{L}(\mathbf{J}_j) \rangle \qquad (21)$$

so that (19) becomes

$$\sum_j Z_{ij} I_j = V_i \quad i = 1, 2, \ldots, N . \qquad (22)$$

Since there are N of these equations they can be written in matrix form

$$[Z]\,[I] = [V] \qquad (23)$$

[Z] is the generalized impedance matrix and [V] is the excitation vector. The vector of unknown current coefficients can be solved for by inverting [Z]

$$[I] = [Z]^{-1}[V] = [Y][V] \quad . \tag{24}$$

The impedance elements are

$$Z_{ij} = \iint_S \mathbf{W}_i \cdot (jw\mathbf{A}_j + \nabla\Phi_j)\,ds \quad . \tag{25}$$

If $\mathbf{W}$ is thought of as a current, the charge associated with it is

$$\rho_i = -\frac{1}{j\omega}\nabla\cdot\mathbf{W}_i \quad . \tag{26}$$

Now (25) can be written as

$$Z_{ij} = j\omega \iint_S (\mathbf{W}_i\cdot\mathbf{A}_j + \rho_i\Phi_j)\,ds \tag{27}$$

or

$$Z_{ij} = \iint_S ds' \iint_s ds\,[j\omega\mu\,\mathbf{W}_i\cdot\mathbf{J}_j + \frac{1}{j\omega\epsilon}(\nabla'\cdot\mathbf{W}_i)(\nabla\cdot\mathbf{J}_j)]\cdot\frac{e^{-jkR}}{4\pi R} \tag{28}$$

where primed donates a source point (associated with $\mathbf{J}_j$) and unprimed a field point (associated with $\mathbf{W}_i$)

C. MM SOLUTION FOR THE SPECIAL CASE OF BODIES OF REVOLUTION

So far the discussion has been for an arbitrary conducting body. In this section we restrict the surfaces to those generated by revolving a plane curve about the z axis. Hence an appropriate set of basis functions are

$$\mathbf{J}^t_{mj} = \mathbf{u}_t f_j^t(t)\, e^{jm\phi} \qquad m = 0, \pm1, \pm2, \ldots, \infty \tag{29}$$

$$\mathbf{J}^\phi_{mj} = \mathbf{u}_t f_j^\phi(t)\, e^{jm\phi} \qquad m = 0, \pm1, \pm2, \ldots, \infty \tag{30}$$

where $\mathbf{u}_t$ and $\mathbf{u}_\phi$ are t-directed and ϕ-directed unit vectors. An example of body of revolution and the coordinate system is shown in Figure 4. Following the method of moments, the electric current J on S is given by

$$\boldsymbol{J} = \sum_{m,j} \left(I_{mj}^{t} \boldsymbol{J}_{mj}^{t} + I_{mj}^{\phi} \boldsymbol{J}_{mj}^{\phi} \right) \quad . \tag{31}$$

For testing functions, Galerkin's method is used ($\mathbf{W}_k = \mathbf{J}_k^*$) so

$$\boldsymbol{W}_{mi}^{t} = \boldsymbol{u}_t f_i(t)\, e^{-jn\phi} \tag{32}$$

$$\boldsymbol{W}_{mi}^{\phi} = \boldsymbol{u}_\phi f_i(t)\, e^{-jn\phi} \tag{33}$$

The $\mathbf{W}_n$ are orthogonal to $\mathbf{J}_m$, $m \neq n$, over 0 to 2π on ϕ, and also to $\mathcal{L}(\mathbf{J}_m)$. Hence, all impedance elements are zero except those for which m = n, and each mode can be treated separately. This is the major simplification introduced by taking advantage of the rotational symmetry of the body. Although the sum over m in equation (31), has an infinite number of terms, it coverges rapidly in most cases and there-fore can be truncated at some value M.

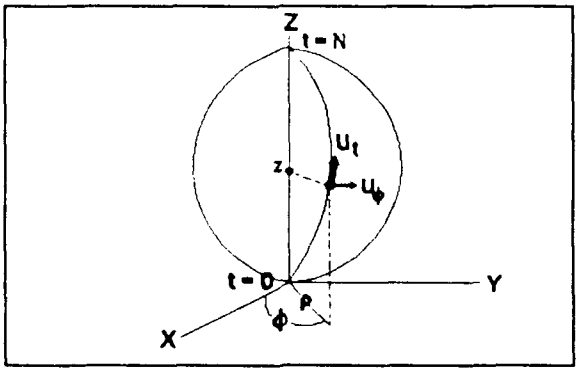

Figure 4: Body of revolution and coordinate system

The use of (29), (30), (32) and (33) to evaluate the elements of (27) results in the matrix equation

$$\begin{bmatrix} [Z_n^{tt}] & [Z_n^{t\phi}] \\ [Z_n^{\phi t}] & [Z_n^{\phi\phi}] \end{bmatrix} \begin{bmatrix} [I_n^t] \\ [I_n^\phi] \end{bmatrix} = \begin{bmatrix} [V_n^t] \\ V_n^\phi] \end{bmatrix} . \tag{34}$$

Here the elements of the submatrices of Z are

$$\begin{aligned} (Z_n^{tt})_{ij} &= \langle \boldsymbol{W}_{ni}^t, \mathcal{L}(\boldsymbol{J}_{nj}^t) \rangle \\ (Z_n^{t\phi})_{ij} &= \langle \boldsymbol{W}_{ni}^t, \mathcal{L}(\boldsymbol{J}_{nj}^\phi) \rangle \\ (Z_n^{\phi t})_{ij} &= \langle \boldsymbol{W}_{ni}^\phi, \mathcal{L}(\boldsymbol{J}_{nj}^t) \rangle \\ (Z_n^{\phi\phi})_{ij} &= \langle \boldsymbol{W}_{ni}^\phi, \mathcal{L}(\boldsymbol{J}_{nj}^\phi) \rangle \end{aligned} \tag{35}$$

the elements of the submatrices V are

$$\begin{aligned} (V_n^t)_i &= \langle \boldsymbol{W}_{ni}^t, \boldsymbol{E}^i \rangle \\ (V_n^\phi)_i &= \langle \boldsymbol{W}_{ni}^\phi, \boldsymbol{E}^i \rangle \end{aligned} \tag{36}$$

and the elements of the submatrices of I are the coefficients in expansion (31). The solution to (34) can be written as

$$\begin{bmatrix} [I_n^t] \\ [I_n^\phi] \end{bmatrix} = \begin{bmatrix} [Y_n^{tt}] & [Y_n^{t\phi}] \\ [Y_n^{\phi t}] & [Y_n^{\phi\phi}] \end{bmatrix} \begin{bmatrix} [V_n^t] \\ [V_n^\phi] \end{bmatrix} . \tag{37}$$

The submatrices of Y are in general obtained after inversion of the entire Z matrix, and not the inverses of the corresponding Z submatrices. The -n mode matrices are related to the +n mode matrices by

$$\begin{bmatrix} [Y_{-n}^{tt}] & [Y_{-n}^{t\phi}] \\ [Y_{-n}^{\phi t}] & [Y_{-n}^{\phi\phi}] \end{bmatrix} = \begin{bmatrix} [Y_n^{tt}] & [-Y_n^{t\phi}] \\ [-Y_n^{\phi t}] & [Y_n^{\phi\phi}] \end{bmatrix} . \tag{38}$$

Hence, only the $n \geq 0$ mode matrices need be inverted.

D. MEASUREMENT MATRICES

Obtaining the scattered field from the current **J** on the body S can be done using a measurement vector

$$measurement = \iint_S \boldsymbol{E}^r \cdot \boldsymbol{J} ds \tag{39}$$

where $\mathbf{E}^r$ is the plane wave field scattered by a differential current element (a known function), which is weighted by the current at every point on S. Since the current is given by (31), (39) reduces to

$$measurement = [R]\,[I] \tag{40}$$

where R is a measurement row vector

$$[R] = [\langle \boldsymbol{J}_j, \boldsymbol{E}^r \rangle] \tag{41}$$

and I is the current vector. Substitution of (24) into (40) gives

$$measurement = [R]\,[Y]\,[V] \ . \tag{42}$$

For bodies of revolution, the expansion for **J** can be separated into t- and ϕ-directed components. Equation (41) becomes

$$\begin{aligned} (R_n^t)_i &= \langle \boldsymbol{J}_{ni}^t, \boldsymbol{E}^r \rangle \\ (R_n^\phi)_i &= \langle \boldsymbol{J}_{ni}^\phi, \boldsymbol{E}^r \rangle \end{aligned} \ . \tag{43}$$

In partitioned form,

$$measurement = [\,[R_n^t]\ [R_n^\phi]\,] \begin{bmatrix} [Y_n^{tt}] & [Y_n^{t\phi}] \\ [Y_n^{\phi t}] & [Y_n^{\phi\phi}] \end{bmatrix} \begin{bmatrix} [V_n^t] \\ [V_n^\phi] \end{bmatrix} \ . \tag{44}$$

A special case is that of the radiation field measurement. Now the **u**-polarized scattered far-field from the current **J** on S is

$$\boldsymbol{E}\cdot\boldsymbol{u} = \frac{-j\omega\mu}{4\pi R} e^{-jkR} [R]\ [I] \tag{45}$$

where the elements of [R] are given by (43) with

$$\boldsymbol{E}^r = \boldsymbol{u} e^{-j\boldsymbol{k}\cdot\boldsymbol{r}} . \tag{46}$$

This is a unit plane wave with polarization vector **u** and propagation vector **k**. An arbitrary plane wave is a superposition of two orthogonal components, for example $\mathbf{E}_\theta$ and $\mathbf{E}_\phi$. Hence, (46) can be treated as two cases, one for $\mathbf{u} = \mathbf{u}_\theta$ and the other for $\mathbf{u} = \mathbf{u}_\phi$. To distinguish between the two cases let

$$\begin{aligned} (R_n^{t\theta})_i &= \langle \boldsymbol{J}_{ni}^t, \boldsymbol{E}_\theta^r \rangle \\ (R_n^{\phi\theta})_i &= \langle \boldsymbol{J}_{ni}^\phi, \boldsymbol{E}_\theta^r \rangle \end{aligned} \tag{47}$$

for the θ-polarized case, and

$$\begin{aligned} (R_n^{t\phi})_i &= \langle \boldsymbol{J}_{ni}^t, \boldsymbol{E}_\phi^r \rangle \\ (R_N^{\phi\phi})_i &= \langle \boldsymbol{J}_{ni}^\phi, \boldsymbol{E}_\phi^r \rangle \end{aligned} \tag{48}$$

for the ϕ-polarized case.

III. METHOD OF MOMENTS SOLUTION FOR THE ADE ANTENNA

A. CALCULATION OF IMPEDANCE ELEMENTS

The mathematical analysis in this section is based on [Ref. 9:p 14-22] and [Ref. 10:p 3-18]. The expansion functions $J_{nj}{}^{t}$ and $J_{nj}{}^{\phi}$, in equation (32), are chosen to be

$$J_{nj}^{t} = u_t \frac{T_j(t)}{\rho} e^{-jn\phi} \qquad \begin{matrix} j=1,2,\ldots,NP-2 \\ n=0,\pm1,\pm2,\ldots,\pm\infty \end{matrix} \tag{49}$$

$$J_{nj}^{\phi} = u_\phi \frac{P_j(t)}{\rho_j} e^{jn\phi} \qquad \begin{matrix} j=1,2,\ldots,NP-1 \\ n=0,\pm1,\pm2,\ldots,\pm\infty \end{matrix} \tag{50}$$

where: u_t, u_ϕ - unit vectors in the t and ϕ direction

n - the mode number

ρ - the distance from the axis of symmetry to a point on the body of revolution

ρ_j - the value of ρ at $t=t_j$ where t_j is the center point of the domain of the pulse

$T_j(t)$ - triangle function shown in Figure 5, which extends over segments j and j+1

$P_j(t)$ - pulse function shown in Figure 6, which extends only over a single segment j.

The purpose of the scale factor $1/\rho_j$ is to give (50) the same dimension as (49). The derivative of $T_j(t)$, which is shown in Figure 8, is also required. The mathematical descriptions of the functions are

$$P_j(t) = 1 \qquad t_j^- \le t \le t_{j+1}^- \tag{51}$$

$$P_j'(t) = \Delta_j \left[\delta\left(t + \left(t_j + \frac{\Delta_j}{2}\right)\right) - \delta\left(t - \left(t_j + \frac{\Delta_j}{2}\right)\right)\right] \tag{52}$$

and

$$T_j(t) = \begin{cases} \dfrac{1}{2} + \dfrac{t - t_j^-}{\Delta_j / 2} & ; \quad t_j^- \le t \le t_{j+1}^- \\ \dfrac{1}{2} - \dfrac{t - t_{j+1}^-}{\Delta_{j+1} / 2} & ; \quad t_{j+1}^- \le t \le t_{j+2}^- \end{cases} \tag{53}$$

$$T_j' = \begin{cases} \dfrac{1}{\Delta_j} & ; \quad t_j^- \le t \le t_{j+1}^- \\ -\dfrac{1}{\Delta_{j+1}} & ; \quad t_{j+1}^- \le t \le t_{j+2} \end{cases} \tag{54}$$

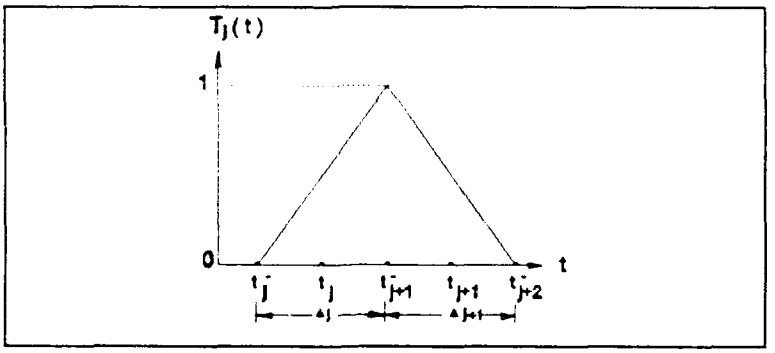

Figure 5: Triangle function $T_j(t)$

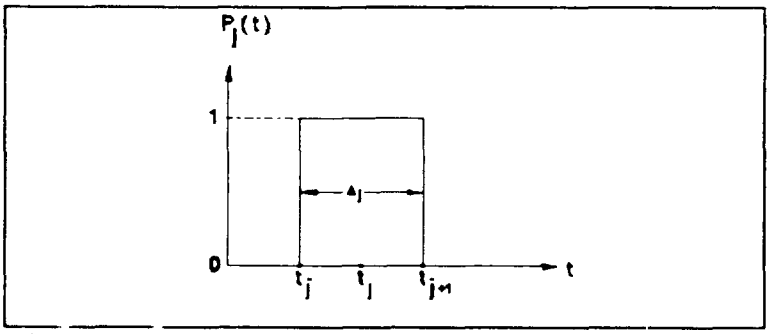

Figure 6: Pulse function $P_j(t)$

In Figures 5,6 and 7, t is the arc length along the body of revolution generating curve and the primes denote differentiation with respect to the argument. It is assumed that the generating curve consists of NP-1 straight line segments where NP is an integer greater than or equal to 3. The j-th segment extends from t_j^- to t_{j+1}^- and has length Δ_j.

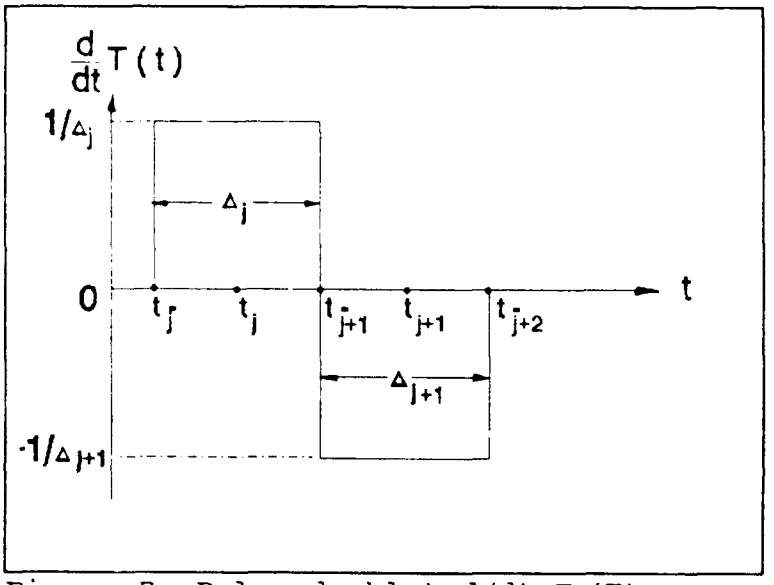

Figure 7: Pulse doublet d/dt $T_j(T)$

For testing functions Galerkin's method is used

$$W_{ni}^t = (J_{ni}^t)^* \tag{55}$$

$$W_{ni}^\phi = (J_{ni}^\phi)^* \tag{56}$$

where * signifies the complex conjugate.

In terms of the basis functions, the current is expressed as

$$J = \sum_{n=-\infty}^{\infty} \left(\sum_{i=1}^{NP-2} I_i^t J_{ni}^t + \sum_{j=1}^{NP-1} I_j^\phi J_{nj}^\phi \right) . \qquad (57)$$

After applying the method of moments testing procedure a matrix equation of the form of equation (25) results

$$I = Z^{-1}V \qquad (58)$$

where

$$\begin{bmatrix} I_1^t \\ I_2^t \\ \cdot \\ \cdot \\ \cdot \\ I_{NP-2}^t \\ I_1^\phi \\ \cdot \\ \cdot \\ \cdot \\ I_{NP-1}^\phi \end{bmatrix} = \mathbf{Z}^{-1} \begin{bmatrix} V_1^t \\ V_2^t \\ \cdot \\ \cdot \\ \cdot \\ V_{NP-2}^t \\ V_1^\phi \\ \cdot \\ \cdot \\ \cdot \\ V_{NP-1}^\phi \end{bmatrix} \qquad (59)$$

I is the vector of current coefficients, V is the excitation vector and Z is the method of moments impedance matrix.

The impedance matrix can be partitioned according to the current and testing function components. For each azimuthal mode

$$Z_n^{ss} = \begin{bmatrix} Z_n^{tt} & Z_n^{t\phi} \\ Z_n^{\phi t} & Z_n^{\phi\phi} \end{bmatrix} . \qquad (60)$$

For convenience let

$$\begin{aligned} MT &= NP-2 \quad (\textit{ number of surface triangles }) \\ MP &= NP-1 \quad (\textit{ number of surface pulses }) \end{aligned} \tag{61}$$

Thus the dimensions of the submatrices of Z are

$$\begin{aligned} Z_n^{tt} &\sim MT \times MT \\ Z_n^{t\phi} &\sim MT \times MP \\ Z_n^{\phi t} &\sim MP \times MT \\ Z_n^{\phi\phi} &\sim MP \times MP \end{aligned} \tag{62}$$

Althought n can take on values between $\pm\infty$, the sum must be truncated to some finite value, M. When multiple modes are used, the complete impedance matrix becomes

$$Z = \begin{bmatrix} Z_{-M}^{ss} & 0 & \cdots & 0 \\ 0 & & \cdots & 0 \\ 0 & & \cdots & 0 \\ 0 & \cdots & Z_0^{ss} & \cdots 0 \\ 0 & & \cdots & 0 \\ 0 & & \cdots & 0 \\ 0 & & \cdots & Z_{+M}^{ss} \end{bmatrix} . \tag{63}$$

Fortunately this a block diagonal matrix; the inverse of Z is also a block diagonal matrix with diagonal submatrices $(Z_n^{ss})^{-1}$.

To explicitly evaluate the impedance elements, the basis and testing functions are used in equation (28)

$$Z_{ij}^{pq} = \frac{jk\eta}{4\pi} \int\int_i ds \int\int_j ds' \frac{e^{-jkR}}{R} \left(\boldsymbol{J}_i^p \cdot \boldsymbol{W}_j^q - \frac{1}{k^2} \left(\nabla_s \cdot \boldsymbol{J}_i^p \right) \left(\nabla_s \cdot \boldsymbol{W}_j^q \right) \right) \tag{64}$$

where p and q signify all possible combinations of t and ϕ, and η is the intrinsic impedance. It is only necessary to evaluate a few of these; the remainder can be obtained by the following mode symmetry

$$\begin{vmatrix} [Z_n^{tt}]_{ij} & [Z_n^{t\phi}]_{ij} \\ [Z_n^{\phi t}]_{ij} & [Z_n^{\phi\phi}]_{ij} \end{vmatrix} = \begin{vmatrix} [Z_n^{tt}]_{ji} & -[Z_n^{\phi t}]_{ji} \\ -[Z_n^{t\phi}]_{ji} & [Z_n^{\phi\phi}]_{ji} \end{vmatrix} \tag{65}$$

and symmetry between positive and negative modes

$$\begin{vmatrix} [Z_{-n}^{tt}]_{ij} & [Z_{-n}^{t\phi}]_{ij} \\ [Z_{-n}^{\phi t}]_{ij} & [Z_{-n}^{\phi\phi}]_{ij} \end{vmatrix} = \begin{vmatrix} [Z_n^{tt}]_{ij} & -[Z_n^{t\phi}]_{ij} \\ -[Z_n^{\phi t}]_{ij} & [Z_n^{\phi\phi}]_{ij} \end{vmatrix} . \tag{66}$$

For a body of revolution

$$\iint_s ds = \int_0^{NP} \rho(t,\phi)\, dt \int_0^{2\pi} d\phi \tag{67}$$

and similarly for the primed integration. The dot products are

$$\boldsymbol{J}_{ni}^{p} \cdot \boldsymbol{W}_{nj}^{q} = e^{jn(\phi'-\phi)} f_i^p(t)\, f_j^q(t')\, \boldsymbol{u}_p \cdot \boldsymbol{u}'_q \ . \tag{68}$$

The functions f_i and f_j are either the pulse or triangle depending on p or q.

The unit vector dot products can be defined in terms of integration variables in Figure 4,

$$\begin{aligned} \mathbf{u}'_t \cdot \mathbf{u}_t &= \sin(v)\sin(v')\cos(\phi-\phi') + \cos(v)\cos(v') \\ \mathbf{u}'_t \cdot \mathbf{u}_\phi &= -\sin(v')\sin(\phi-\phi') \\ \mathbf{u}'_\phi \cdot \mathbf{u}_t &= \sin(v)\sin(\phi-\phi') \\ \mathbf{u}'_\phi \cdot \mathbf{u}_\phi &= \cos(\phi-\phi') \end{aligned} \tag{69}$$

Here v is the angle between the t direction and the Z-axis, being positive if $\mathbf{u}_t$ points away from the Z-axis and negative if $\mathbf{u}_t$ points toward it. Using equations (51), (52), (53) and (54), the elements of Z are given by

$$(Z_n^{tt})_{ij} = j\int_{t_i^-}^{t_{i+2}^-} dt \int_{t_j^-}^{t_{j+2}^-} dt' \left(kT_i(t)\, T_j(t')\, (G_1 \sin(v)\sin(v') + G_3\cos(v)\cos(v')) - G_3 \frac{d}{dt} T_i(t)\, \frac{d}{dt'} T_j(t')\right) \tag{70}$$

$$(Z_n^{\phi t})_{ij} = -\frac{1}{\rho_i}\int_{t_i^-}^{t_{i+1}^-} dt\, P_i(t) \int_{t_j^-}^{t_{j+1}^-} dt' \left(k\rho\, T_j(t')\, G_2 \sin(v') + nG_3 \frac{d}{dt'} T_j(t')\right) \tag{71}$$

$$(Z_n^{t\phi})_{ij} = \frac{1}{\rho_j}\int_{t_i^-}^{t_{i+2}^-} dt \int_{t_j^-}^{t_{j+1}^-} dt' P_j(t') \left(k\rho' T_i(t)\, G_2 \sin(v) + nG_3 \frac{d}{dt} T_i(t)\right) \tag{72}$$

$$(Z_n^{\phi\phi})_{ij} = \frac{j}{\rho_i \rho_j}\int_{t_i^-}^{t_{i+1}^-} dt\; P_i(t) \int_{t_j^-}^{T_{j+1}^-} dt' P_j(t') \left(k\rho\rho' G_1 - n^2 G_3\right) \tag{73}$$

where

$$G_0 = 2\int_0^{\pi} d\phi\, \frac{e^{-jkR}}{kR} \sin^2\left(\frac{\phi}{2}\right) \cos(n\phi) \tag{74}$$

$$G_1 = \int_0^{\pi} d\phi\, \frac{e^{-jkR}}{kR} \cos(\phi)\cos(n\phi) \tag{75}$$

$$G_2 = \int_0^{\pi} d\phi \, \frac{e^{-jkR}}{kR} \sin(\phi) \sin(n\phi) \tag{76}$$

$$G_3 = G_0 + G_1 = \int_0^{\pi} d\phi \, \frac{e^{-jkR}}{kR} \cos(n\phi) \tag{77}$$

$$R = \sqrt{(\rho' - \rho)^2 + (z' - z)^2 + 4\rho\rho' \sin^2\left(\frac{\phi}{2}\right)} \; . \tag{78}$$

The parameters ρ, z, and v depend on t, while ρ', z',and v' depend on t'.

To reduce the number of numerical integrations, the δ-function approximation is used for the integral with respect to t in (70) - (73)

$$\int_{t_p^-}^{t_{p+1}^-} f(t)\, dt \approx f(t_p)\, \Delta_p \tag{79}$$

where f(t) is the relevant integrand and, as indicated in Figures 6 and 7,

$$t_p = \frac{1}{2}\left(t_p^- + t_{p+1}^-\right) \tag{80}$$

$$\Delta_p = \left(t_{p+1}^- - t_p^-\right) \; . \tag{81}$$

Application of (79) to (70) - (73), leaves only one integral with respect to t in each equation. These are evaluated numerically as are the integrals with respect to ϕ in the G functions defined earlier. Another integration shortcut is achieved by noting that when testing is performed,

the integrals in adjacent impedance elements that span a common segment are the opposite of each other. Thus, for the impedance elements

$$(\hat{Z}_n^{tt})_{ij} = j\Delta_p \int_{t_q^-}^{t_{q+1}^-} dt' (k t_i(t_p)\, T_j(t')\, (G_1 \sin(v_p) \sin(v') + G_3 \cos(v_p) \cos(v')) - G_3 \left[\frac{d}{dt} T_i(t)\right]_{t_p} \frac{d}{dt'} T_j(t') \tag{82}$$

$$(\hat{Z}_n^{\phi t})_{pj} = -\Delta_p P_p(t_p) \int_{t_q^-}^{t_{q+1}^-} dt' \left(k T_j(t') G_2 \sin(v') + \frac{n}{\rho_p} G_3 \frac{d}{dt'} T_j(t')\right) \tag{83}$$

$$(\hat{Z}_n^{t\phi})_{iq} = \Delta_p \int_{t_q^-}^{t_{q+1}^-} dt' P_q(t') \left(\frac{k\rho'}{\rho_p} T_i(t_p)\, G_2 \sin(v_p) + \frac{n}{\rho_q} G_3 \left[\frac{d}{dt} T_i(t)\right]_{t_p}\right) \tag{84}$$

$$(Z_n^{\phi\phi})_{pq} = j\Delta_p P_p(t_p) \int_{t_q^-}^{t_{q+1}^-} dt' P_q(t') \left(\frac{k\rho'}{\rho_q} G_1 - \frac{n^2}{\rho_p \rho_q} G_3\right) . \tag{85}$$

The ^ denotes the contribution due to integration over the region A_{pq}, and therefore i is p-1 or p and j is q-1 or q. Note that all the unprimed quantities that depend on t are now evaluated at $t=t_p$ due to the approximate integration method. Further substitution for the functions P(t) and T(t) give the final equations

$$(\hat{Z}_n^{tt})_{ij} = j\frac{k\Delta_p\Delta_q}{8})\,(G_{1a}\sin(v_p)\sin(v_q) + G_{3a}\cos(v_p)\cos(v_q)) + \frac{(-1)^{q-j}jk\Delta_p\Delta_q}{8}(G_{1b}\sin(v_p)\sin(v_q) + G_{3b}\cos(v_p)\cos(v_q) - \frac{(-1)^{p+q-i-j)}}{2}jG_{3a} \quad (86)$$

$$(\hat{Z}_n^{\phi t})_{pj} = -(\frac{k\Delta_p\Delta_q\sin(v_q)}{4})\,G_{2a} - (-1)^{q-j}((\frac{k\Delta_p\Delta_q\sin(v_q)}{4})\,G_{2b} + (\frac{n\Delta_p}{2\rho_p})\,G_{3a}) \quad (87)$$

$$(\hat{Z}_n^{t\phi})_{iq} = (\frac{k\Delta_p\Delta_q\sin(v_p)}{4})\,(G_{2a} + \frac{\Delta_q\sin(v_q)}{2\rho_q}G_{2b}) + (-1)^{p-i}(\frac{n\Delta_q}{2\rho_q})\,G_{3a} \quad (88)$$

$$(Z_n^{\phi\phi})_{pq} = 2j[(\frac{k\Delta_p\Delta_q}{4})\,(G_{1a} + \frac{\Delta_q\sin(v_q)}{2\rho_q}G_{1b}) - (\frac{n\Delta_q}{2\rho_q})\,(\frac{n\Delta_p}{2\rho_p})\,G_{3a} \quad (89)$$

$$G_{1a} = \frac{2}{\Delta_q}\int_{t_q^-}^{t_{q+1}^-} G_m(t' - t_q)\,dt' \qquad m = 0, 1, 2 \quad (90)$$

$$G_{1b} = (\frac{2}{\Delta_q})^2\int_{t_q^-}^{t_{q+1}^-} (t' - t_q)\,G_m(t' - t_q)\,dt' \qquad m = 0, 1, 2\ . \quad (91)$$

Substitution of R_p for R in (75) - (77) gives

$$G_0(t' - t_q) = 2\int_0^{\pi} d\phi\,\frac{e^{-jkR_p}}{kR_p}\sin^2(\frac{\phi}{2})\cos(n\phi) \quad (92)$$

$$G_1(t' - t_q) = \int_0^{\pi} d\phi\,\frac{e^{-jkR_p}}{kR_p}\cos(\phi)\cos(n\phi) \quad (93)$$

$$G_2(t'-t_q) = \int_0^{\pi} d\phi \frac{e^{-jkR_p}}{kR_p} \sin(\phi) \sin(n\phi) \qquad (94)$$

where R_p is

$$R_p = \sqrt{(\rho'-\rho_p)^2 + (z'-z_p)^2 + 4\rho_p\rho'\sin^2(\frac{\phi}{2})} \ . \qquad (95)$$

Evaluation of the integrals in (92) through (94) is done using n_t-point Gaussian quadrature

$$\int_a^b f(x)\,dx \approx \frac{b-a}{2}\sum_{m=1}^{n_t} c_m f(\alpha_m) \qquad (96)$$

$$\alpha_m = \frac{b-a}{2} x_m + \frac{b+a}{2} \qquad (97)$$

where c_m are the weights and x_m are the zeros of the Legendre polynomials. Typically $n_t = 2$ is sufficient for the t'-integration. For the ϕ-integration the appropriate value depends on the maximum radial extent of the surface. (An approximate rule of thumb is 10 points per wavelength of circumference.) The calculated values of G_m are substituted into (92) and (93) in order to evaluate G_{ma} and G_{mb}. The resulting values of G_{ma} and G_{mb} are then substituted into (86) - (89) to evaluate the elements of the impedance matrix.

The general MM solution can be applied to multiple detached surfaces as in the ADE antenna. The extension to multiple surfaces is primarily a bookkeeping problem that complicates the computer code. A simple way of calculating the

current on multiple bodies is to perform the calculation as if they were attached and then set the appropriate impedance and excitation elements to zero.

Figure 8 shows the two reflector surfaces of the ADE antenna connected by a fictitious "dummy segment." After the Z-matrix calculation, any element that spans the m^{th} segment is set to zero, as shown in Figure 9 for the case of triangular basis functions and Figure 10 for pulses.

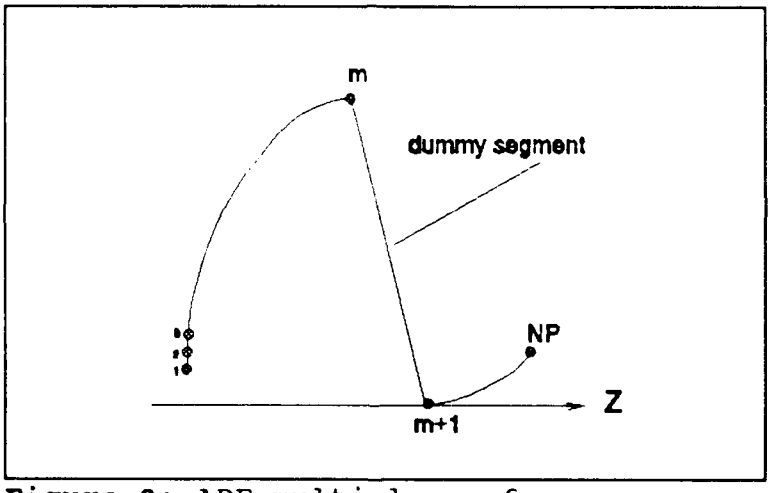

Figure 8: ADE multiple surfaces

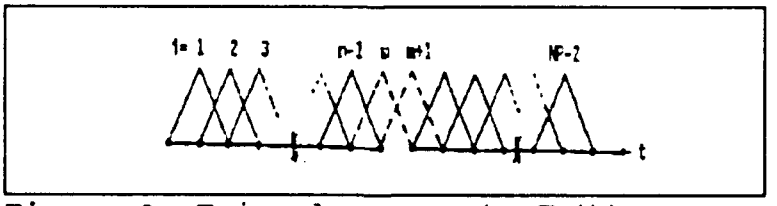

Figure 9: Triangle segments $T_j(t)$

To avoid a singular matrix the diagonals of the zeroed rows and columns are set to 1. The final matrix structure is

illustrared in Figure 11. This method does not use computer memory efficiently, but is suitable for antennas with only a few detached surfaces.

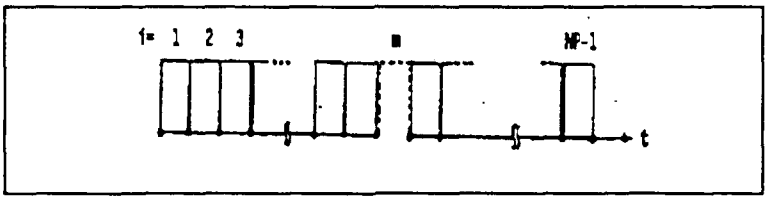

Figure 10: Pulse segments - $P_j(t)$

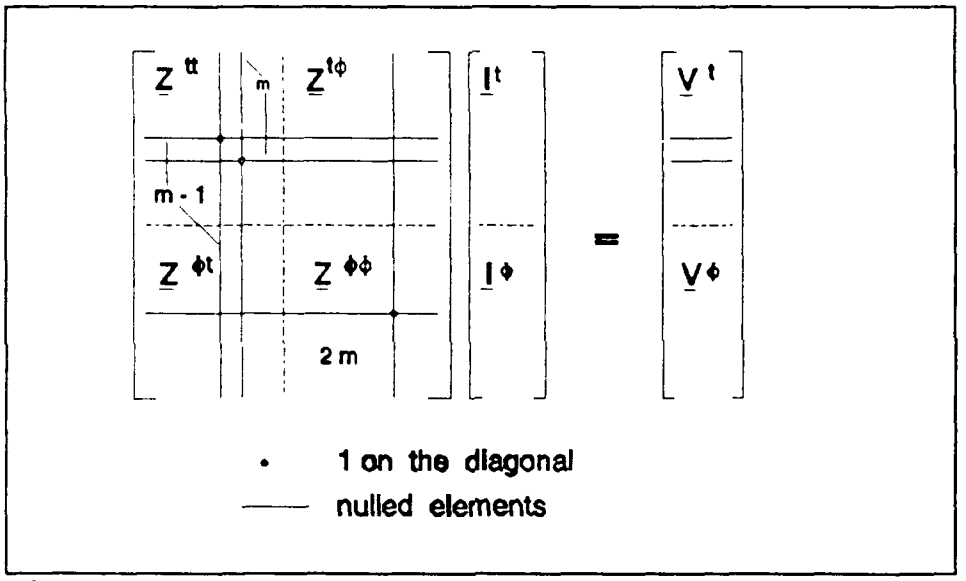

Figure 11: Resulting impedance matrix for multiple scatterers

B. EVALUATION OF THE EXCITATION VECTOR

The excitation vector for a θ or ϕ-polarized wave incident in the ϕ=0 plane is defined by

$$\mathbf{E}^{inc}_{\theta,\phi} = \mathbf{u}^{t}_{\theta,\phi}\, k\eta\, e^{-j\mathbf{k}_t\cdot\mathbf{r}} \qquad (98)$$

where

$$\boldsymbol{k}_t = -k\left(\boldsymbol{u}_x \sin(\theta_t) + \boldsymbol{u}_z \sin(\theta_t)\right) \qquad (99)$$

$$\mathbf{u}_\phi = \mathbf{u}_y \tag{100}$$

$$\mathbf{u}_\theta = \mathbf{u}_x \cos(\theta_t) - \mathbf{u}_z \sin(\theta_t) \ . \tag{101}$$

θ_t is the angle of incidence and $\mathbf{u}_x$, $\mathbf{u}_y$, and $\mathbf{u}_z$ are unit vectors in the x, y, and z directions. $\mathbf{r}$ is the position vector from the origin to the test point on the body. The elements $\mathbf{V}_n^{t,\phi}$ are given by

$$V_{ni}^{t,\phi} = \frac{1}{\eta} \iint_S \mathbf{W}_{ni}^{t,\phi} \cdot \mathbf{E}^i \, ds \ . \tag{102}$$

A detailed development of the excitation vector can be found in [Ref. 10: p 27-31]. The final results are obtained by substituting (98) - (101) in (102). Using the same notation developed earlier

$$\hat{V}_{ni}^{t\phi} = \frac{j^{n+1}\pi k \Delta_p \sin(v_p)\cos(\phi_t)}{4}(F_{n+1,a} - F_{n-1,a}) - \frac{j^n \pi k \Delta_p \cos(v_p)\sin(\phi_t)}{2} F_{na}$$
$$+ (-1)^{p-i}\{\frac{j^{n+1}\pi k \Delta_p \sin(v_p)\cos(\phi_t)}{4}(F_{n+1,b} - F_{n-1,b})$$
$$- \frac{j^n \pi k \Delta_p \cos(v_p)\sin(\phi_t)}{2} F_{nb}\} \tag{103}$$

$$V_{np}^{\phi\theta} = \frac{j^n \pi k \Delta_p \cos(\theta_t)}{2}\left((F_{n+1,a} + F_{n-1,a}) + \frac{\Delta_p \sin(v_p)}{2\rho_p}(F_{n+1,b} + F_{n-1,b})\right) \tag{104}$$

$$V_{np}^{\phi\phi} = \frac{j^{n+1}\pi k \Delta_p}{2}\left((F_{n+1,a} - F_{n-1,a}) + \frac{\Delta_p \sin(v_p)}{2\rho_p}(F_{n+1,b} - F_{n-1,b})\right) \tag{105}$$

$$\hat{V}_{ni}^{t\phi} = -\frac{j^n \pi k \Delta_p \sin(v_p)}{4} (F_{n+1,a} + F_{n-1,a}) - \frac{(-1)^{p-i} j^n \pi k \Delta_p \sin(v_p)}{4} \cdot (F_{n+1,b} + F_{n-1,b}) \quad . \tag{106}$$

New functions have been defined in (103) - (106),

$$F_{ma} = \frac{2}{\Delta_p} \int_{t_p^-}^{t_{p+1}^-} J_m(k\rho \sin(\phi_t))\, e^{-jkz\cos(\phi_t)}\, dt \quad ; \quad m = n-1, n, n+1 \tag{107}$$

$$F_{mb} = \left(\frac{2}{\Delta_p}\right)^2 \int_{t_p^-}^{t_{p+1}^-} (t - t_p)\, J_m(k\rho \sin(\theta_t))\, e^{jkz\cos(\theta_t)}\, dt \quad ; \quad m = n-1, n, n+1 \tag{108}$$

$J_m(k\rho\sin(\theta_t))$ is the m-th order Bessel function, which results from the integration in ϕ, and

$$\rho = \rho_p + (t - t_p) \sin(v_p) \tag{109}$$

$$z = z_p + (t - t_p) \cos(v_p) \quad . \tag{110}$$

The remaining integrations are evaluated using a Gaussian quadrature formula as in the case of the impedance elements.

At this point all of the quantities required to solve the method of moments matrix equation have been defined. An existing computer code, originally developed by Mautz and Harrington, was modified to compute these elements for the ADE antenna. The computer code operation is described in the following chapter.

IV. COMPUTER PROGRAM

In this section, the FORTRAN program which implements the numerical solution of CHAPTER III is discussed (the computer listing is given in Appendix A). The program consists of a MAIN PROGRAM and the subroutines ZMAT, SPHERE, PLANE, PLAN, DECOMP, SOLVE and the functions BLOG, ETHETA, EPHI.

The main program obtains the radiation pattern and gain of an ADE antenna for an ideal feed at body of revolution coordinate system origin. The subroutine SPHERE calculates the elements of excitation vector in (23) for spherical wave incidence. The subroutine ZMAT calculates the elements of the moment matrix in (24). The function BLOG is called by ZMAT. The subroutines DECOMP and SOLVE solve the matrix equation (24) for $I_n^{t,\phi}$. The subroutine PLANE calculates the plane wave receive vector elements need to obtain the radiation field.

A. THE MAIN PROGRAM

The main program is divided to two main parts. The ADE ANTENNA RADIATION PATTERN (lines 1 - 334) and the GAIN PROGRAM(lines 335 - 453). Both parts are based on Mautz and Harrington's computer program for bodies of revolution.

1. The ADE Antenna Radiation Pattern

This portion of the main program computes the radiation pattern of an ADE type of antenna. An ideal feed (a

point source with a directive pattern) is at BOR coordinate system origin and therefore only n = ±1 are required. Lines 17 - 73 are basic initializations including integration coefficients for the ϕ-integration (NPHI) in lines 31 - 37, and integration points for the t-integration (NT) in lines 43 - 48. The antenna geometry is defined in lines 49 - 59: the total number of generating points (NP), the number of the main reflector points (NP1) and the number of the subreflector points (NP2). Lines 60 - 73 define the feed pattern which is of the form

$$\boldsymbol{E}_{feed} = \frac{e^{-jkR}}{R} \left(\hat{\theta}\cos^{n}(\theta)\cos(\phi) + \hat{\phi}\cos^{m}(\theta)\sin(\phi)\right) \qquad \textbf{(111)}$$

where n = FEXP and m = FHXP in the code. The simple case of a Lambertian source is n,m = 1.

The next portion (74 - 211) of this part of the program generates an array of surface contour points for calculating the moment matrix and the excitation vector. Lines 74 - 113 define the antenna parameters which are discussed in Chapter I. To create the contour of the main reflector (which is paraboloid), ψ is varied in the equation

$$R_m = \frac{2f}{1 + \cos(\psi)} \; . \qquad \textbf{(112)}$$

ψ is the polar angle from the paraboloid vertex and R_m is the distamce from the focus to the surface point at angle ψ. The coordinates of the surface are

$$\rho = R_m \cos(\psi)$$
$$z = R_m \sin(\psi) \quad . \tag{113}$$

For the subreflector (which is ellipsoid),

$$F_s = \frac{AA\,(1 - ECC^2)}{1 \pm ECC \cdot \cos(\theta)} \quad . \tag{114}$$

The values of kρ and kz are stored in the arrays RH and ZH.

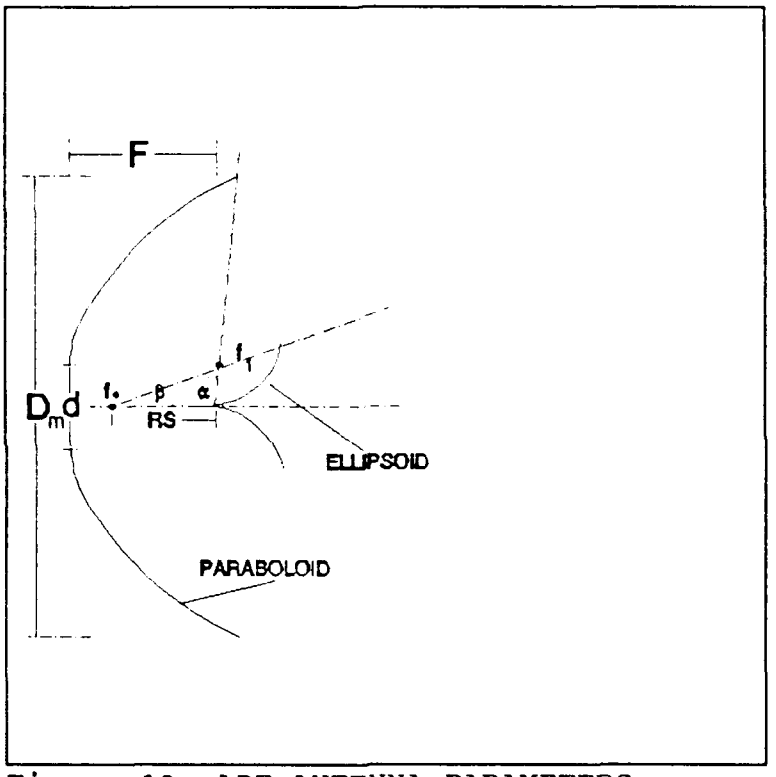

Figure 12: ADE ANTENNA PARAMETERS

After ZH and RH are determined, the program calls the SPHERE subroutine to calculate the excitation coefficients and ZMAT to get the moment matrix. Next, lines 212 - 226 take care of the "dummy segment" between multiple surfaces, mentioned in the previous chapter. In lines 227- 240 the subroutines DECOMP

and SOLVE solve the matrix equation (24) for I_n^t and I_n^ϕ, and in the lines 241 - 334 the far field patterns in the E and H planes are computed according to equations (40) - (49).

2. Gain Program

The second half of the main program calculates the gain and the efficiency of the ADE antenna. Far field pattern integration, based on the previously calculated currents, are used to get the total radiated power. Lines 345 - 360 are initialization and specifying integration coefficients for the ϕ (NPHI) and t (NT) integrations. A normalization is loop incorporated in lines 351 - 382 to obtain $\mathbf{E}_{max}$. In lines 383 - 402 the θ and ϕ-integration intervals are defined
The directivity is computed from the formula

$$\Omega_A = \int_0^{2\pi}\int_0^{\pi} |E(\theta,\phi)|^2 R^2 SIN(\theta)\, d\theta\, d\phi \qquad (115)$$

$$DIRECTIVITY = \frac{4\pi\, |E_{max}|^2}{\Omega_A} \qquad (116)$$

where $\mathbf{E}(\theta,\phi)$ is the total electric field (i.e., that radiated by the feed plus that scattered from the reflector). $\mathbf{E}_{max}$ is obtained from the normalization loop.

B. THE SUBROUTINE SPHERE

The subroutine SPHERE computes the spherical wave excitation vector for the body of revolution. The source is assumed to be located at the origin of the BOR coordinate

system. The arguments are defined in the program. It returns R, a column vector of length N containing V^t and V^ϕ for mode n = +1, in that order.

C. THE SUBROUTINE ZMAT

The subroutine ZMAT calculates the moment matrix in (23) for n = 1 and stores them in Z, which is the only output argument. The storage of the Z_n submatrices in Z is as follows:

$$\begin{aligned}
(Z_n^{tt})_{ij} &\in Z(i+N*(j-1)) \\
(Z_n^{\phi t})_{ij} &\in Z(i+N*(j-1) + NP-2) \\
(Z_n^{t\phi})_{ij} &\in Z(i+N*(j-1) + (NP-2)*N) \\
(Z_n^{\phi\phi})_{ij} &\in Z(i+N*(j-1) + (NP-2)*N+NP-2)
\end{aligned} \qquad \textbf{(117)}$$

where N=2*NP-3. More details about the ZMAT subroutine can be found in [Ref. 10: p. 43-56].

D. THE SUBROUTINES DECOMP AND SOLVE

The subroutines DECOMP and SOLVE solve a system of N linear equation in N unknowns. The input to DECOMP consist of N and the N by N matrix of coefficients on the left-hand side of the matrix equation stored by columns in Z. The output from DECOMP is IPS and Z. The output is fed into SOLVE. The rest of the input to SOLVE consists of N and the column of coefficients on the right-hand side of the matrix equation stored in B. The solution to the matrix equation is in X. Further details concerning DECOMP and SOLVE can be found in [Ref. 13: p. 46 - 49].

E. THE SUBROUTINES PLANE AND PLAN

The subroutines PLAN and PLANE are essentially the same and compute the plane wave receive and excitation vectors for the BOR according to (103) - (106). They are stored in R which is the only output argument. The rest of the arguments of PLANE and PLAN are input arguments and have all been defined previously, except NF which is always 1 as implemented here. The receive vectors are returned in the following order: $R^{t\theta}$, $R^{\phi\theta}$, $R^{t\phi}$, $R^{\phi\phi}$. These subroutines were written by Mautz and Harrington, and are described in detail in [Ref. 12: p. 57 - 62].

V. COMPUTED RESULTS

An evaluation of practical ADE antenna configurations has been performed using the MM computer code. The main reflector diameter was 6" at 44 GHZ (22.352 wavelength), which was chosen the same as the M.I.T-LINCOLN Lab design [Ref. 6]. A second fixed parameter was the focal length to main reflector diameter ratio (FOD) which was 0.15. The displacement distance from the axis of symmetry to inside edge of the main reflector is (d). The ratio of (d) to the main reflector diameter (dOD) was fixed at 0.2. The edge angle of the paraboloid (ALPHA) is equal to 105°. The subreflector edge angle and the eccentricity (or equivalently, the feed location, Rf) were varied. The range of design parameters that was investigated are summerized in Table 1. For each of these antennas the gain was calculated. The gain was referred to that of a uniformly illuminated unblocked aperture to arrive at an efficiency. Because MM includes all of the interactions between the surfaces, all of the loss mechanisms (edge diffractions, surface waves, multiple reflections, etc.) are considered. Only the feed is assumed to be ideal.

Three typical reflector configurations are shown in Figures 13, 14, and 15. The principal plane patterns are given in Figures 16, 17 and 18. The optimum occured for BETA = 45°. For smaller values of BETA the spillover increased. For larger

values of BETA the subreflector edge begins to turn back on itself, which causes edge diffraction to increase and some partial blocking of the wave reflected from the paraboloid.

TABLE 1

ADE INVESTIGATED PARAMETERS

PARAMETER	RANGE OF VALUES
DM	22.352λ
FOD	0.15
dOD	0.2
ALPHA	105°
BETA	30° to 55°
Rf	0.25λ to 2.75λ

The subreflector shape also affects the radiation in the rear hemisphere (the backlobe). The computer code assumes that there is a hole of diameter d in the center of the main reflector. According to ray optices, there will be no energy passing through the hole. In this case the subreflector is rather small in terms of wavelengths, so its scattered field is not very directive. Therefore some energy reflected from the ellipsoid will pass through the hole. The effect is more noticeable when the subreflector projected area is larger, as in the case of larger BETAs.

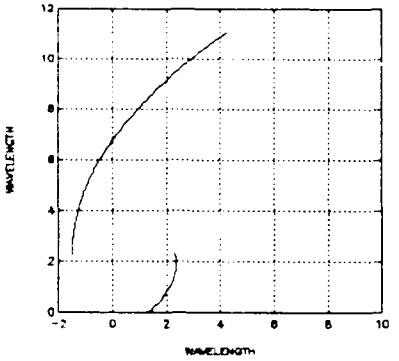

Figure 13: ADE ANTENNA SHAPE FOR BETA=45°

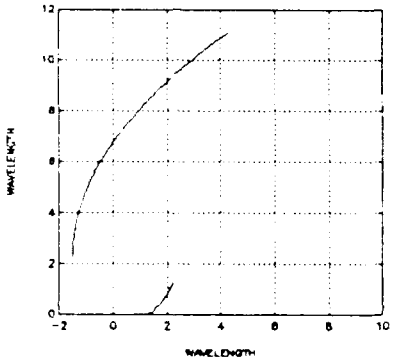

Figure 14: ADE ANTENNA SHAPE FOR BETA=30°

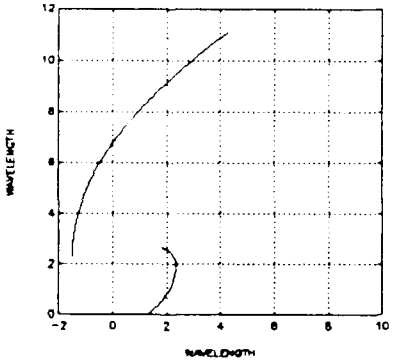

Figure 15: ADE ANTENNA SHAPE FOR BETA=55°

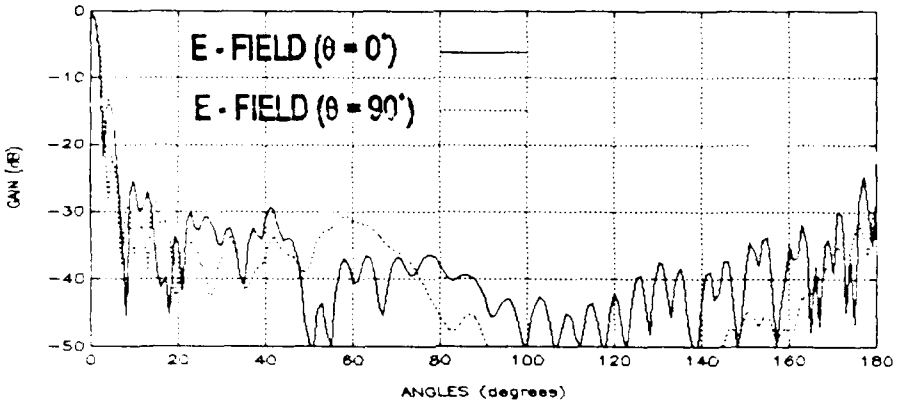

Figure 16: E-FIELD RADIATION PATTERN FOR BETA=45°

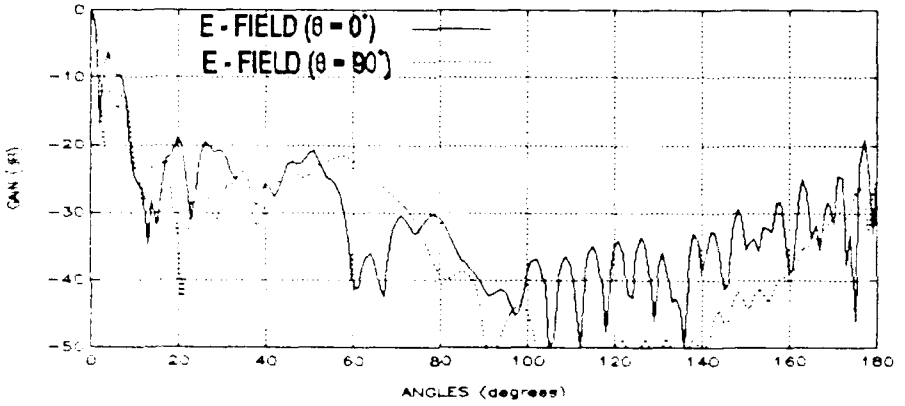

Figure 17: E-FIELD RADIATION PATTERN FOR BETA=30°

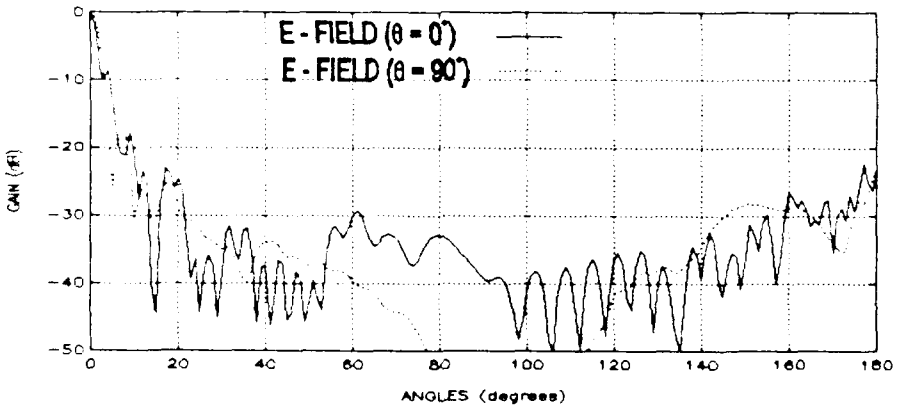

Figure 18: E-FIELD RADIATION PATTERN FOR BETA=55°

The effect of moving the feed point along the axis of symmetry was investigated. In practice it is desireable to have the feed as close to the main reflector as possible. This reduces the transmission line length and also minimizees the interaction between the feed and subreflector. However, the subreflector edge angle is smaller in this case and there will be more spillover. Spillover is the primary contributor in reducing the gain of small dual reflector antennas. To reduce spillover requires a larger feed (narrower beamwidth) which in turn increases the interaction between the feed and subreflector. The subreflector will be in the near field of a large feed, so the illumination amplitude and phase will not be uniform. The distance of the feeder from the main reflector was changed from 0.25 wavelength to 2.75 wavelength in increments of a quarter wavelength. At the same time, for each value of Rf, the subreflector edge angle (BETA) was changed from 30° to 55°. The eccentricity is directly related to the feeder location (there is one-to-one correspondence). The goal was to optimize the efficiency over all of the parameter ranges described above. The results are summerized in Figure 19. The highest efficiency is 48.3% for a Lambertian feed ($COS(\theta)$), when it is located at 1.5 wavelengths from the main reflector with BETA is 45°.

A second investigation was performed to examine the effect of the feed directivity. The shape of the theoretical feeder was changed from $COS(\theta)$ to $COS^2(\theta)$. The geometric parameters

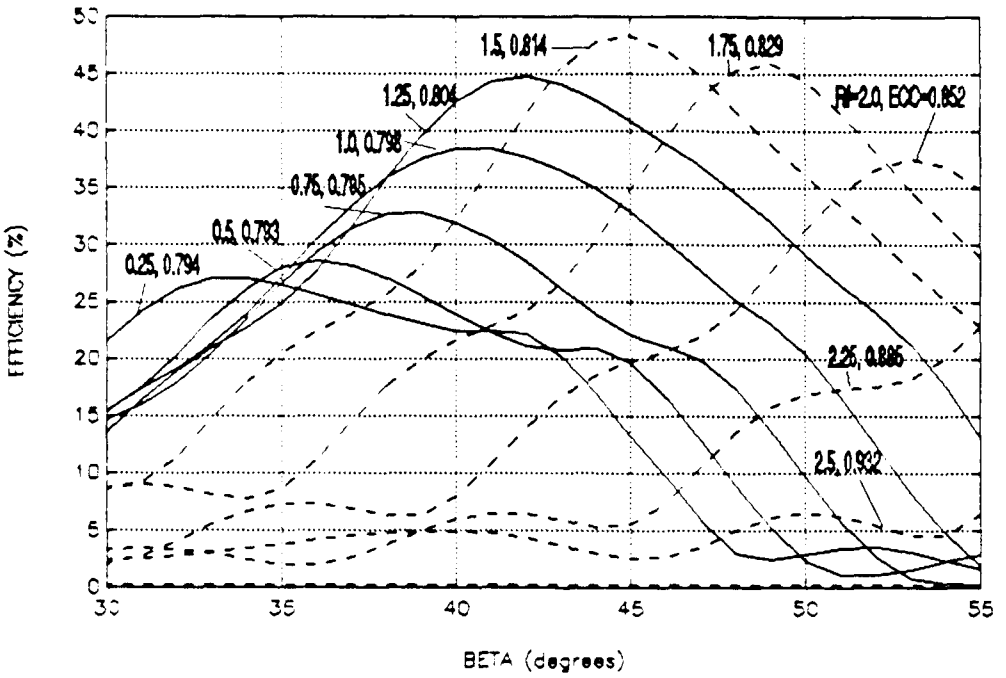

Figure 19: SUBREFLECTOR SHAPING VERSUS EFFICIENCY FOR DIFFERENT FEEDER LOCATIONS (COS(θ))

were varied through the same range as in the case of Figure 19. As expected, by increasing the feed directivity the efficiency has been improved. However, the optimum configuration remained the same. The assumed ideal feed pattern can be integrated directly to find the spillover energy. This was done for the optimum configuration (48.3% efficiency) and the spillover loss was to found to be 3 dB. Removing this loss from the 48.3% gives 96.6%, showing that the feed spillover is indeed the major source of energy loss.

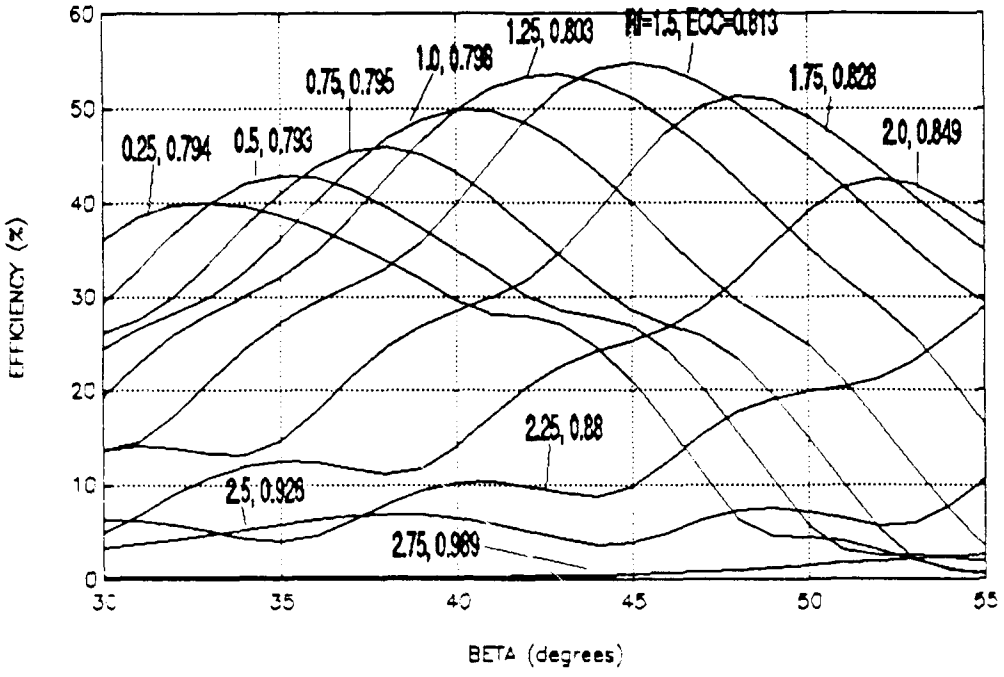

Figure 20: SUBREFLECTOR SHAPING VS. EFFICIENCY FOR DIFFERENT FEEDER LOCATIONS ($COS^2(\theta)$)

VI. SUMMARY AND CONCLUSIONS

In the previous chapters the EFIE was derived for conducting surfaces and then specialized to multiple surfaces of revolution with the ADE shape. A computer program was written to solve for currents, far field radiation pattern, gain and efficiency. Efficiency as a function of subreflector shape (BETA) and the feeder location, was investigated for various feed directivities.

The computed results that were obtained were predicable. Maximum efficiency for an ideal source such as Lambertian was 48.3% for 6" diameter ADE antenna at 44 GHZ. The first sidelobe level was -12 dB below the main beam. The second sidelobe was -25 dB down at angle of 9° from the main lobe, which is at the same location measured in [Ref. 6]. The results show how the far-out sidelobes drop off rapidly, which helps to reduce interference from outside sources which are not located close to the main beam. The back lobe radiation varies with the subreflector shape because of the hole at the center of the main reflector. It is in the -25 dB range relative to the main lobe which is typical for this small reflector size. The efficiency of the ADE is higher than that of a Cassegrain antenna of the same size and feed illumination.

The computed and measured patterns for the configuration of [Ref. 6] are for a dual band feed, which was not included in the computed results. The program neglects feed interactions with the reflector surfaces. In [Ref. 6.] a circular waveguide is located very close to the subdish. Hence the results are noticeably different for both the gain and efficiency. However, it has been demonstrated that the program gives an optimum point for the antenna geometry that is relatively insensitive to the feed pattern. This provides a starting point for the antenna design process. Once a particular feed is selected, a development model can be built and optimized by tuning the feed to minimize the feed and subreflector interactions.

The next logical step is to include a more accurate feed model into the antenna code so that the interactions between it and the other surfaces are accounted for. Simple feeds can be modeled directly; more complicated feeds can be simulated using measured data. Since the subreflector often lies in the near field of the feed, a spherical wave expansion representation of the measured feed field should be used.

The use of low-blockage feed types such as dipoles and parasitic elements should be investigated. These types of feeders will minimize the interaction between the feed and subdish and can be included by slightly changing the program.

APPENDIX

COMPUTER CODES

```
C   *ADE ANTENNA RADIATION PATTERN*
C
C  RADIATION PATTERN OF AN ADE ANTENNA
C  BASED ON MAUTZ AND HARRINGTON'S COMPUTER PROG FOR BORS.
C  SPHERICAL SOURCE IS AT BOR COORDINATE SYSTEM ORIGIN.
C  (THIS IMPLIES n=+1,-1 ARE THE ONLY TWO NONZERO MODES.)
C  VARIABLE FEED EXPONENT; GAIN AND SPILLOVER LOSS ARE
C  COMPUTED
C
C   ICALC=0 CALC CURRENTS AND FIELD
C        =1 CALC FIELDS ONLY (READ CURRENTS)
C   ICWRT=0 WRITE CURRENTS ON DISC FILE
C    ISEG=0 PRINT SURFACE SEGMENT POINTS
C  IPRINT=0 PRINT TABLE OF FAR FIELD POINTS -- OTHERWISE ONLY
C           GAIN AND SPILLOVER ARE PRINTED
C
      COMPLEX EP,ET,Z(300000),R(4000),B(2000),C(2000),U,UC
      COMPLEX ETT,EPT,ETST,ETSP,EPST,EPSP,EC,EX
      DIMENSION RH(2000),ZH(2000),XT(10),AT(10),IPS(500)
      DIMENSION AG(100),A(300),X(300),EXP(1200),ANG(1000)
      DIMENSION ECP(1000),XG(100),ECV(1000),EXV(1000)
      DIMENSION PHC(1000),PHX(1000),Q(30),S(30)
      DATA PI,START,STOP,DT/3.14159,0.,180.,1./
      DATA ICALC/0/,ISEG/0/,IPRINT/0/,ICWRT/0/
      DATA NT/2/,XT(1),AT(1)/.5773503,1./
C     DATA NT/4/,XT(1),XT(2),AT(1),AT(2)/.33998104,
C    *.8611363115,.6521451548,.3478548451/
C
C     READ GAUSSIAN CONSTANTS
C
      OPEN(1,FILE='/home/srv1/vered/thesis/outgaus',
     *STATUS='old')
      READ(1,*) NPHI
      DO 3 K=1,NPHI
      READ(1,*) X(K),A(K)
    3 CONTINUE
      CLOSE(1)
      RAD=PI/180.
      BK=2.*PI
      U=(0.,1.)
      U0=(0.,0.)
      UC=-U/4./PI
      NT2=NT/2
      DO 1 K=1,NT2
```

```
      K1=NT-K+1
      AT(K1)=AT(K)
      XT(K1)=XT(K)
    1 XT(K)=-XT(K)
C
C NP1=NUMBER OF MAIN REFLECTOR PTS.; NP2=NUMBER OF
C SUBREFLECTOR PTS.
C
      NP1=91
      NP2=19
      NP=NP1+NP2
      MP=NP-1
      MT=MP-1
      N=MT+MP
      write(6,*) 'np,n=',np,n
C
C SPECIFY FEED PATTERN WHICH IN OUR CASE IS LAMBERTIAN WITH
C N=1 AND IS LOCATED AT THE ORIGIN.
C
C FEED FUNCTION EXPONENT:
C       ETHETA=COS(THETA)**FEXP*COS(PHI)
C       EPHI=COS(THETA)**FHXP*SIN(PHI)
C
      FEXP=1.0
      FE2=2.*FEXP+1.
      FHXP=1.0
      FH2=2.*FHXP+1.
      DIR=2.*FE2*FH2/(FEXP+FHXP+1.)
      PRAD=1./FE2+1./FH2
C
C READ THE ADE INPUT PARAMETERS:
C
C DM=MAIN REFLECTOR DIAMETER (PARABOLOID)
C Rfeed=THE DISTANCE BETWEEN THE FEEDER AND THE MAIN REFLECTOR
C
C FOD=THE RATIO BETWEEN THE FOCUS AND THE DIAMETER OF THE MAIN
C    REFLECTOR
C d/2=DISTANCE BETWEEN THE EDGE OF THE MAIN REFLECTOR AND THE
C    AXIS OF SYMMETRY
C dOD=THE RATIO BETWEEN THE ABOVE d AND THE MAIN REFLECTOR
C    DIAMETER
C ALPHA=THE ANGLE BETWEEN THE LOWER EDGE OF THE SUBREFLECTOR
C     TO THE SECOND FOCUS (NOT THE ORIGIN)
C BETA=THE ANGLE BETWEEN THE AXIS OF SYMMETRY AND THE
C IMAGINARY LINE BETWEEN THE ORIGIN TO THE EDGE OF THE
C SUBREFLECTOR
C ECC=ECCENTRICITY OF THE SUBREFLECTOR (ELLIPSOID)
C
C
C                    FIRST  GENERATE  PARABOLOID  CONTOUR
C
```

```
      WRITE(6,*) 'ENTER ALPHA'
      READ(5,*) ALPHA
      WRITE(6,*) 'ENTER BETA'
      READ(5,*) BETA
      WRITE(6,*) 'ENTER DM (IN WAVELENGTH)'
      READ(5,*) DM
      WRITE(6,*) 'FOD'
      READ(5,*) FOD
      WRITE(6,*) 'dOD'
      READ(5,*) dOD
      ALPHA=ALPHA*RAD
      BETA=BETA*RAD
      FM=FOD*DM
      d=dOD*DM
      Rmax=FM-d/2./TAN(PI-ALPHA)
      WRITE(6,*) 'MAXIMUM FEEDER DISTANCE IS', Rmax
      WRITE(6,*) 'ENTER Rfeed (IN WAVELENGTH)'
      READ(5,*) Rfeed
C
C FM=FOCUS OF THE MAIN REFLECTOR (PARABOLOID)
C ZSHIFT=INITIALIZE THE ORIGIN TO BE AT ZERO
C
      ZSHIFT=FM-Rfeed
      DO 5 I=1,NP1
      TH=FLOAT(I-1)*ALPHA/FLOAT(NP1-1)
      RM=2.*FM/(1.+COS(TH))
      ZH(I)=(ZSHIFT-RM*COS(TH))*BK
      RH(I)=(d/2.+RM*SIN(TH))*BK
5     CONTINUE
C
C          SUBREFLECTOR  CONTOUR
C
      PHIZ=ATAN(d/2./ZSHIFT)
      DELTA=PI-ALPHA-PHIZ
      CPZ=COS(PHIZ)
      CPS=COS(BETA)
      BB=2*SIN(DELTA)/SIN(ALPHA)
      AA=bb*COS(PHIZ)-1
      ECC=(BB-SQRT(BB**2-4*(AA)))/2/AA
      WRITE(6,*) 'ECCENTRICITY =',ECC
      EDGEE=CPS**(FEXP*2.)
      EDGEH=CPS**(FHXP*2.)
      EEDB=10.*ALOG10(EDGEE)
      EHDB=10.*ALOG10(EDGEH)
      PSPILL=FH2*(1.-EDGEE)+FE2*(1.-EDGEH)
      PSPILL=PSPILL/(FH2+FE2)
      PSDB=10.*ALOG10(PSPILL)
      DO 6 I=1,NP2
      THETA=FLOAT(I-1)*(BETA)/FLOAT(NP2-1)
      RSS=AA*((1.-ECC**2.)/(1.-ECC*COS(PHIZ-THETA)))*BK
      ZH(I+NP1)=RSS*COS(THETA)
```

```
      RH(I+NP1)=RSS*SIN(THETA)
6     CONTINUE
      OPEN(8,file='/home/srv1/vered/thesis/outADE')
      WRITE(8,8000) DM,RS,ECC,PHIZ/RAD,ALPHA/RAD,NP1,NP2,FEXP,
     * FHXP
 8000 FORMAT(//,5X,'*** ADE ANTENNA SYSTEM ***',//,5X,
     *'REFLECTOR PARAMETERS (LENGTHS IN WAVELENGTHS):',/,5X,
     *'MAIN REFL DIA=',F8.3,/,5X,'SUB REFL DISTANCE=',F8.3,/,
     *5X,'ECCENTRICITY=',F8.4,/,5X,'PHIZ (DEG)=',F8.2,/,5X,
     *'ALPHA (DEG)=',F8.2,/,5X,'MAIN REFL POINTS (NP1)=',I4,/,
     *5X,'SUB REFL POINTS (NP2)=',I4,/,5X,'E-PLANE FEED
     *EXPONENT=',F8.3,/,5X,'H-PLANE FEED EXPONENT=',F8.3)
      WRITE(8,30) NT,NPHI
   30 FORMAT(/,7X,' NT   NPHI',/,5X,I5,2X,I5)
      IF(ISEG.EQ.0) WRITE(8,1300)
 1300 FORMAT(/,5X,'INDEX',8X,'Z(I)',10X,'RHO(I)')
      OPEN(1,file='/home/srv1/vered/matlab/zeem.m')
      OPEN(2,file='/home/srv1/vered/matlab/rhom.m')
      OPEN(3,file='/home/srv1/vered/matlab/zees.m')
      OPEN(4,file='/home/srv1/vered/matlab/rhos.m')
      DO 52 I=1,NP
      IF(ABS(ZH(I)).LT..001) ZH(I)=0.
      IF(ABS(RH(I)).LT..001) RH(I)=0.
      ZHB=ZH(I)/BK
      RHB=RH(I)/BK
      IF(I.LE.NP1) THEN
      WRITE(1,31) ZHB
      WRITE(2,31) RHB
      ENDIF
      IF(I.GE.NP1+1) THEN
      WRITE(3,31) ZHB
      WRITE(4,31) RHB
      ENDIF
51    if(iseg.eq.0) WRITE(8,8004) I,ZHB,RHB
52    CONTINUE
8004  FORMAT(6X,I4,4X,F8.3,8X,F8.3)
31    FORMAT(F8.4)
      CLOSE(1)
      CLOSE(2)
      CLOSE(3)
      CLOSE(4)
      write(6,*) 'geometry defined'
      IF(ICALC.EQ.1) THEN
      open(3,file='/home/srv1/vered/thesis/current')
      READ(3,*) DM0,DS0,FC0,PHIV0,PHIR0
      READ(3,*) ECC0,FOD0,NP10,NP20,FEXP0,FHXP0
      WRITE(6,*)DM0,DS0,FC0,PHIV0,PHIR0,ECC0,FOD0,NP10,NP20,
     *FEXP0
      WRITE(6,*) DM,DS,FC,PHIV,PHIR,ECC,FOD,NP1,NP2,FEXP
      READ(3,*) (RH(J),J=1,NP)
      READ(3,*) (ZH(J),J=1,NP)
```

```
      READ(3,*) (C(J),J=1,N)
      WRITE(6,*) 'CURRENTS READ SUCCESSFULLY'
      CLOSE(3)
      ENDIF
      IF(ICALC.EQ.0) THEN
      CALL SPHERE(FEXP,FHXP,NP1,NP2,NT,RH,ZH,XT,AT,BK,R)
      DO 22 J=1,N
      B(J)=R(J)
      IF(J.GT.MT) B(J)=-B(J)
   22 CONTINUE
      write(6,*) 'excitation coefficients computed'
      ENDIF
      CALL ZMAT(1,1,NP1,NP2,NPHI,NT,RH,ZH,X,A,XT,AT,Z)
      write(6,*) 'back from zmat'
C
C NULL OUT ROWS AND COLUMNS CORRESPONDING TO DUMMY SEGMENTS
C
      DO 700 LSS=1,N
      LS=LSS-1
      Z(LS*N+NP1)=(0.,0.)
      Z(LS*N+NP1-1)=(0.,0.)
  700 Z(LS*N+NP1+MT)=(0.,0.)
      DO 701 LS=1,N
      Z((NP1-2)*N+LS)=(0.,0.)
      Z((NP1-1)*N+LS)=(0.,0.)
  701 Z((NP1-1+MT)*N+LS)=(0.,0.)
      Z((NP1-2)*N+NP1-1)=(1.,0.)
      Z((NP1-1)*N+NP1)=(1.,0.)
      Z((MT+NP1-1)*N+NP1+MT)=(1.,0.)
      CALL DECOMP(N,IPS,Z)
      CALL SOLVE(N,IPS,Z,B,C)
      write(6,*) 'coefficients calculated'
      IF(ICWRT.EQ.0) THEN
      OPEN(3,file='/home/srv1/vered/thesis/current')
      WRITE(3,*) DM,DS,FC,PHIV,PHIR,ECC
      WRITE(3,*) FOD,NP1,NP2,FEXP,FHXP
      WRITE(3,*) (RH(J),J=1,NP)
      WRITE(3,*) (ZH(J),J=1,NP)
      WRITE(3,*) (C(J),J=1,N)
      CLOSE(3)
      ENDIF
  991 CONTINUE
      IT=INT((STOP-START)/DT)+1
C
C RECEIVER PHI CUTS: DO 0 AND 90 (E- AND H- PLANES)
C
      DO 400 IP=1,2
      ECX=0.
      PHI=0.
      IF(IP.EQ.2) PHI=90.
      PHR=PHI*RAD
```

```
      CNP=COS(PHR)
      SNP=SIN(PHR)
      DO 500 I=1,IT
      THETA=FLOAT(I-1)*DT+START
      THX=THETA*RAD
      CALL PLANE(1,1,NP1,NP2,NT,RH,ZH,XT,AT,THX,R)
      ETST=(0.,0.)
      EPST=(0.,0.)
      ETSP=(0.,0.)
      EPSP=(0.,0.)
      DO 100 I0=1,MT
      ETST=ETST+R(I0)*C(I0)
  100 ETSP=ETSP+R(I0+N)*C(I0)
      DO 200 I0=1,MP
      EPST=EPST+R(I0+MT)*C(I0+MT)
  200 EPSP=EPSP+R(I0+N+MT)*C(I0+MT)
      ETF=CNP*FE(FEXP,THX)
      EPF=SNP*FH(FHXP,THX)
      ETT=2.*(ETST+EPST)*UC*CNP
      EPT=2.*U*(ETSP+EPSP)*UC*SNP
      ET=ETF+ETT
      EP=EPF+EPT
      EC=(ET*CNP-EP*SNP)
      EX=(ET*SNP+EP*CNP)
      ECV(I)=CABS(EC)
      EXV(I)=CABS(EX)
      ECR=REAL(EC)
      ECI=AIMAG(EC)
      EXR=REAL(EX)
      EXI=AIMAG(EX)
      PHC(I)=ATAN2(ECI,ECR+1.e-10)/RAD
      PHX(I)=ATAN2(EXI,EXR+1.e-10)/RAD
      ANG(I)=THETA
      ECX=AMAX1(ECX,ECV(I),EXV(I))
  500 CONTINUE
      IF(IP.EQ.1) THEN
      WRITE(8,103) ECX,EEDB,EHDB,PSPILL,PSDB
  103 FORMAT(/,5X,'E-PLANE EDGE TAPER=',F8.2,
     * /,5X,'H-PLANE EDGE TAPER=',F8.2,/,5X,'TOTAL RAD
     * POWER=',E15.5,
     * /,5X,'SPILLOVER LOSS =',F8.4,/,5X,'          IN dB
     * =',f8.2)
      ENDIF
      WRITE(8,107) PHI
  107 FORMAT(/,5X,'PHI OF RECEIVER (DEG)=',F8.2)
      DO 600 I=1,IT
      ECP(I)=(ECV(I)/ECX)**2
      EXP(I)=(EXV(I)/ECX)**2
      ECP(I)=AMAX1(ECP(I),.00001)
      EXP(I)=AMAX1(EXP(I),.00001)
      ECP(I)=10.*ALOG10(ECP(I))
```

```
      EXP(I)=10.*ALOG10(EXP(I))
  600 CONTINUE
      IF(IPRINT.NE.0) GO TO 300
      WRITE(8,5015)
 5015 FORMAT(/,7X,'ANGLE',15X,'CO-POL',25X,'X-POL',/,7X,
     1'(DEG)',4X,2('(VOLTS)',4X,'(DEG)',3X,'(DB-REL)',4X))
      DO 9000 L=1,IT
      WRITE(8,5016)ANG(L),ECV(L),PHC(L),ECP(L),EXV(L),PHX(L)
     1,EXP(L)
 5016 FORMAT(5X,F6.1,3X,2(F8.2,3X,F7.1,3X,F7.2,3X))
 9000 CONTINUE
  300 CONTINUE
      IF(IP.EQ.1) THEN
      OPEN(2,file='/home/srv1/vered/matlab/cang.m')
      OPEN(3,file='/home/srv1/vered/matlab/ccpole.m')
      OPEN(4,file='/home/srv1/vered/matlab/cxpole.m')
      DO 9097 I=1,IT
      WRITE(2,5019) ANG(I)
      WRITE(3,5019) ECP(I)
 9097 WRITE(4,5019) EXP(I)
      CLOSE(2)
      CLOSE(3)
      CLOSE(4)
      ENDIF
      IF(IP.EQ.2) THEN
      OPEN(3,file='/home/srv1/vered/matlab/ccpolh.m')
      OPEN(4,file='/home/srv1/vered/matlab/cxpolh.m')
      DO 9098 I=1,IT
      WRITE(3,5019) ECP(I)
 9098 WRITE(4,5019) EXP(I)
      CLOSE(3)
      CLOSE(4)
      ENDIF
400   CONTINUE
5019  FORMAT(F8.3)
C
C program gain.f
C
C FAR FIELD PATTERN INTEGRATION FOR LOSS CALCULATIONS.
C USES THE PREVIOUSLY CALCULATED CURRENTS TRANSFERRED FROM
C pardip.f.
C   *** general wire/bor geometries can be handled ***
C   >>>> INPUT FILE IS current
C   >>>> HAS A GAIN NORMALIZATION LOOP INCORPORATED
C
      OPEN(1,FILE='/home/srv1/vered/thesis/outgaus')
      READ(1,*) NPHI
      NT2=NT/2
      DO 7 K=1,NT2
      K1=NT-K+1
      AT(K1)=AT(K)
```

```
      XT(K1)=XT(K)
    7 XT(K)=-XT(K)
      DO 8 K=1,NPHI
    8 READ(1,*) XG(K),AG(K)
      NDIVT=1
      NDIVP=1
      S1=0.
      S2=180.
      Q1=0.
      Q2=180.
C
C GAIN NORMALIZATION LOOP (USE THETA=PHI=0 AND THETA POL)
C
      CNP=1.
      CALL PLAN(1,1,NP,NT,RH,ZH,XT,AT,0.,R)
      ETST=(0.,0.)
      EPST=(0.,0.)
      DO 101 I0=1,MT
  101 ETST=ETST+R(I0)*C(I0)
      DO 201 I0=1,MP
  201 EPST=EPST+R(I0+MT)*C(I0+MT)
      ETT=2.*(ETST+EPST)*UC*CNP
      ETF=CNP*FE(FEXP,0.)
      ET=ETT+ETF
      EMAX=CABS(ET)
      WRITE(6,*) 'EMAX=',EMAX
      WRITE(8,8008) NT,NPHI,NDIVP,NDIVT,S1,S2,Q1,Q2
 8008 FORMAT(//,10X,'NT=',I3,/,10x,'NPHI=',I4,/,10X,
     * 'NUMBER OF INTEGRATION INTERVALS IN PHI=',i3,/,10x,
     * 'NUMBER OF INTEGRATION INTERVALS IN THETA=',i3,/,10x,
     * 'THETA LIMITS: START,STOP=',F7.2,2X,F7.2,/,10X,
     * 'PHI LIMITS: START,STOP=',F7.2,2X,F7.2)
c
c theta integration intervals
c
      S1=S1*RAD
      S2=S2*RAD
      Q1=Q1*RAD
      Q2=Q2*RAD
      DS=(S2-S1)/FLOAT(NDIVT)
      DO 502 I=1,NDIVT+1
      S(I)=(I-1)*DS
      WRITE(6,*) "I,S(I)=",I,S(I)
  502 CONTINUE
c
c phi integration intervals
c
      DQ=(Q2-Q1)/FLOAT(NDIVP)
      DO 503 I=1,NDIVP+1
      Q(I)=(I-1)*DQ
      WRITE(6,*) "I,Q(I)=",I,Q(I)
```

```
 503 CONTINUE
     SUM=0.
     do 2000 JJ=1,NDIVP
     P1=DQ/2.
     P2=(Q(JJ+1)+Q(JJ))/2.
     DO 2000 J=1,NPHI
     PHR=p1*xg(j)+p2
     DO 1000 II=1,NDIVT
     T1=DS/2.
     T2=(S(II+1)+S(II))/2.
     DO 1000 I=1,NPHI
     THR=T1*XG(I)+T2
     IF(THR.LT.PI) GO TO 510
     THR=(BK-THR)
     PHR=PHR+PI
 510 CONTINUE
     SNP=SIN(PHR)
     CNP=COS(PHR)
     CALL PLAN(1,1,NP,NT,RH,ZH,XT,AT,THR,R)
     STRA=SIN(THR)*AG(I)*AG(J)
     ETST=(0.,0.)
     EPST=(0.,0.)
     ETSP=(0.,0.)
     EPSP=(0.,0.)
     DO 104 I0=1,MT
     ETST=ETST+R(I0)*C(I0)
 104 ETSP=ETSP+R(I0+N)*C(I0)
     DO 204 I0=1,MP
     EPST=EPST+R(I0+MT)*C(I0+MT)
 204 EPSP=EPSP+R(I0+N+MT)*C(I0+MT)
     ETT=2.*(ETST+EPST)*UC*CNP
     EPT=2.*U*(ETSP+EPSP)*UC*SNP
     ETF=CNP*FE(FEXP,THR)
     EPF=SNP*FH(FHXP,THR)
     ET=ETT+ETF
     EP=EPT+EPF
     SUM=SUM+(CABS(ET)**2+CABS(EP)**2)*STRA
1000 CONTINUE
2000 CONTINUE
     PRAD=T1*P1*SUM
     GAIN=2.*PI*EMAX**2/PRAD
     GDB=10.*alog10(GAIN)
     EFF=GAIN/(PI*DM)**2.*100.
     WRITE(8,8010) PRAD,EMAX,GAIN,GDB,EFF
8010 FORMAT(//,10X,'TOTAL RADIATED POWER=',E15.8,/,10X,
    * 'MAXIMUM FIELD VALUE (V/M)=',E15.8,/,10X,
    * 'GAIN=',E15.8,/,10x,'(dB)=',f8.2,
    * 'EFFICIENCY=',E15.8,2x,'%')
     WRITE(6,*)"PRAD,GAIN,dB=,EFFICIENCY",PRAD,GAIN,GDB,EFF
  32 FORMAT(F8.4)
9999 STOP
```

```
      END
      SUBROUTINE ZMAT(M1,M2,NP1,NP2,NPHI,NT,RH,ZH,X,A,XT,AT,Z)
C
C subroutine to compute the impedance elements for BORs.
C Original version from Mautz and Harrington (Improved E-Field
C Method ...)
C THE SUBROUTINE ZMAT CALLS THE FUNCTION BLOG
C
      COMPLEX U1,U2,U3,U4,U5,U6,U7,U8,U9,UA,UB,G4A(10),G5A(10)
      COMPLEXG6A(10),G4B(10),G5B(10),G6B(10),H4A,H5A,H6A,H4B
      COMPLEX CMPLX,H6B,UC,UD,GA(100),GB(100),H5B,Z(300000)
      DIMENSION RH(300),ZH(300),X(100),A(100),XT(10),AT(10)
      DIMENSION RS(300),ZS(300),D(300),DR(300),DZ(300)
      DIMENSION DM(300),C2(100),C3(100),R2(10),Z2(10),R8(10)
      DIMENSION C4(100),C5(100),C6(100),Z7(10),R7(10),Z8(10)
      NP=NP1+NP2
      CT=2.
      CP=.1
      DO 10 I=2,NP
      I2=I-1
      RS(I2)=.5*(RH(I)+RH(I2))
      ZS(I2)=.5*(ZH(I)+ZH(I2))
      D1=.5*(RH(I)-RH(I2))
      D2=.5*(ZH(I)-ZH(I2))
      D(I2)=SQRT(D1*D1+D2*D2)
      DR(I2)=D1
      DZ(I2)=D2
      IF(RS(I2).EQ.0.) RS(I2)=1.
      DM(I2)=D(I2)/RS(I2)
   10 CONTINUE
      M3=M2-M1+1
      M4=M1-1
      PI2=1.570796
      DO 11 K=1,NPHI
      PH=PI2*(X(K)+1.)
      C2(K)=PH*PH
      SN=SIN(.5*PH)
      C3(K)=4.*SN*SN
      A1=PI2*A(K)
      D4=.5*A1*C3(K)
      D5=A1*COS(PH)
      D6=A1*SIN(PH)
      M5=K
      DO 29 M=1,M3
      PHM=(M4+M)*PH
      A2=COS(PHM)
      C4(M5)=D4*A2
      C5(M5)=D5*A2
      C6(M5)=D6*SIN(PHM)
      M5=M5+NPHI
   29 CONTINUE
```

```
 11 CONTINUE
    MP=NP-1
    MT=MP-1
    N=MT+MP
    N2N=MT*N
    N2=N*N
    U1=(0.,.5)
    U2=(0.,2.)
    JN=-1-N
    DO 15 JQ=1,MP
    KQ=2
    IF(JQ.EQ.1) KQ=1
    IF(JQ.EQ.MP) KQ=3
    R1=RS(JQ)
    Z1=ZS(JQ)
    D1=D(JQ)
    D2=DR(JQ)
    D3=DZ(JQ)
    D4=D2/R1
    D5=DM(JQ)
    SV=D2/D1
    CV=D3/D1
    T6=CT*D1
    T62=T6+D1
    T62=T62*T62
    R6=CP*R1
    R62=R6*R6
    DO 12 L=1,NT
    R2(L)=R1+D2*XT(L)
    Z2(L)=Z1+D3*XT(L)
 12 CONTINUE
    U3=D2*U1
    U4=D3*U1
    DO 16 IP=1,MP
    R3=RS(IP)
    Z3=ZS(IP)
    R4=R1-R3
    Z4=Z1-Z3
    FM=R4*SV+Z4*CV
    PHM=ABS(FM)
    PH=ABS(R4*CV-Z4*SV)
    D6=PH
    IF(PHM.LE.D1) GO TO 26
    D6=PHM-D1
    D6=SQRT(D6*D6+PH*PH)
 26 IF(IP.EQ.JQ) GO TO 27
    KP=1
    IF(T6.GT.D6) KP=2
    IF(R6.GT.D6) KP=3
    GO TO 28
 27 KP=4
```

```
 1      28 GO TO (41,42,41,42),KP
 2      42 DO 40 L=1,NT
 3         D7=R2(L)-R3
 4         D8=Z2(L)-Z3
 5         Z7(L)=D7*D7+D8*D8
 6         R7(L)=R3*R2(L)
 7         Z8(L)=.25*Z7(L)
 8         R8(L)=.25*R7(L)
 9      40 CONTINUE
10         Z4=R4*R4+Z4*Z4
11         R4=R3*R1
12         R5=.5*R3*SV
13         DO 33 K=1,NPHI
14         A1=C3(K)
15         RR=Z4+R4*A1
16         UA=0.
17         UB=0.
18         IF(RR.LT.T62) GO TO 34
19         DO 35 L=1,NT
20         R=SQRT(Z7(L)+R7(L)*A1)
21         SN=-SIN(R)
22         CS=COS(R)
23         UC=AT(L)/R*CMPLX(CS,SN)
24         UA=UA+UC
25         UB=XT(L)*UC+UB
26      35 CONTINUE
27         GO TO 36
28      34 DO 37 L=1,NT
29         R=SQRT(Z8(L)+R8(L)*A1)
30         SN=-SIN(R)
31         CS=COS(R)
32         UC=AT(L)/R*SN*CMPLX(-SN,CS)
33         UA=UA+UC
34         UB=XT(L)*UC+UB
35      37 CONTINUE
36         A2=FM+R5*A1
37         D9=RR-A2*A2
38         R=ABS(A2)
39         D7=R-D1
40         D8=R+D1
41         D6=SQRT(D8*D8+D9)
42         R=SQRT(D7*D7+D9)
43         IF(D7.GE.0.) GO TO 38
44         A1=ALOG((D8+D6)*(-D7+R)/D9)/D1
45         GO TO 39
46      38 A1=ALOG((D8+D6)/(D7+R))/D1
47      39 UA=A1+UA
48         UB=A2*(4./(D6+R)-A1)/D1+UB
49      36 GA(K)=UA
50         GB(K)=UB
51      33 CONTINUE
```

```
      K1=0
      DO 45 M=1,M3
      H4A=0.
      H5A=0.
      H6A=0.
      H4B=0.
      H5B=0.
      H6B=0.
      DO 46 K=1,NPHI
      K1=K1+1
      D6=C4(K1)
      D7=C5(K1)
      D8=C6(K1)
      UA=GA(K)
      UB=GB(K)
      H4A=D6*UA+H4A
      H5A=D7*UA+H5A
      H6A=D8*UA+H6A
      H4B=D6*UB+H4B
      H5B=D7*UB+H5B
      H6B=D8*UB+H6B
   46 CONTINUE
      G4A(M)=H4A
      G5A(M)=H5A
      G6A(M)=H6A
      G4B(M)=H4B
      G5B(M)=H5B
      G6B(M)=H6B
   45 CONTINUE
      IF(KP.NE.4) GO TO 47
      A2=D1/(PI2*R1)
      D6=2./D1
      D8=0.
      DO 63 K=1,NPHI
      A1=R4*C2(K)
      R=R4*C3(K)
      IF(R.LT.T62) GO TO 64
      D7=0.
      DO 65 L=1,NT
      D7=D7+AT(L)/SQRT(Z7(L)+A1)
   65 CONTINUE
      GO TO 66
   64 A1=A2/(X(K)+1.)
      D7=D6*ALOG(A1+SQRT(1.+A1*A1))
   66 D8=D8+A(K)*D7
   63 CONTINUE
      A1=.5*A2
      A2=1./A1
      D8=-PI2*D8+2./R1*(BLOG(A2)+A2*BLOG(A1))
      DO 67 M=1,M3
      G5A(M)=D8+G5A(M)
```

```
 1      67 CONTINUE
 2         GO TO 47
 3      41 DO 25 M=1,M3
 4         G4A(M)=0.
 5         G5A(M)=0.
 6         G6A(M)=0.
 7         G4B(M)=0.
 8         G5B(M)=0.
 9         G6B(M)=0.
10      25 CONTINUE
11         DO 13 L=1,NT
12         A1=R2(L)
13         R4=A1-R3
14         Z4=Z2(L)-Z3
15         Z4=R4*R4+Z4*Z4
16         R4=R3*A1
17         DO 17 K=1,NPHI
18         R=SQRT(Z4+R4*C3(K))
19         SN=-SIN(R)
20         CS=COS(R)
21         GA(K)=CMPLX(CS,SN)/R
22      17 CONTINUE
23         D6=0.
24         IF(R62.LE.Z4) GO TO 51
25         DO 62 K=1,NPHI
26         D6=D6+A(K)/SQRT(Z4+R4*C2(K))
27      62 CONTINUE
28         Z4=3.141593/SQRT(Z4/R4)
29         D6=-PI2*D6+ALOG(Z4+SQRT(1.+Z4*Z4))/SQRT(R4)
30      51 A1=AT(L)
31         A2=XT(L)*A1
32         K1=0
33         DO 30 M=1,M3
34         U5=0.
35         U6=0.
36         U7=0.
37         DO 32 K=1,NPHI
38         UA=GA(K)
39         K1=K1+1
40         U5=C4(K1)*UA+U5
41         U6=C5(K1)*UA+U6
42         U7=C6(K1)*UA+U7
43      32 CONTINUE
44         U6=D6+U6
45         G4A(M)=A1*U5+G4A(M)
46         G5A(M)=A1*U6+G5A(M)
47         G6A(M)=A1*U7+G6A(M)
48         G4B(M)=A2*U5+G4B(M)
49         G5B(M)=A2*U6+G5B(M)
50         G6B(M)=A2*U7+G6B(M)
51      30 CONTINUE
```

```
 13 CONTINUE
 47 A1=DR(IP)
    UA=A1*U3
    UB=DZ(IP)*U4
    A2=D(IP)
    D6=-A2*D2
    D7=D1*A1
    D8=D1*A2
    JM=JN
    DO 31 M=1,M3
    FM=M4+M
    A1=FM*DM(IP)
    H5A=G5A(M)
    H5B=G5B(M)
    H4A=G4A(M)+H5A
    H4B=G4B(M)+H5B
    H6A=G6A(M)
    H6B=G6B(M)
    U7=UA*H5A+UB*H4A
    U8=UA*H5B+UB*H4B
    U5=U7-U8
    U6=U7+U8
    U7=-U1*H4A
    U8=D6*H6A
    U9=D6*H6B-A1*H4A
    UC=D7*(H6A+D4*H6B)
    UD=FM*D5*H4A
    K1=IP+JM
    K2=K1+1
    K3=K1+N
    K4=K2+N
    K5=K2+MT
    K6=K4+MT
    K7=K3+N2N
    K8=K4+N2N
    GO TO (18,20,19),KQ
 18 Z(K6)=U8+U9
    IF(IP.EQ.1) GO TO 21
    Z(K3)=Z(K3)+U6-U7
    Z(K7)=Z(K7)+UC-UD
    IF(IP.EQ.MP) GO TO 22
 21 Z(K4)=U6+U7
    Z(K8)=UC+UD
    GO TO 22
 19 Z(K5)=Z(K5)+U8-U9
    IF(IP.EQ.1) GO TO 23
    Z(K1)=Z(K1)+U5+U7
    Z(K7)=Z(K7)+UC-UD
    IF(IP.EQ.MP) GO TO 22
 23 Z(K2)=Z(K2)+U5-U7
    Z(K8)=UC+UD
```

```
      GO TO 22
   20 Z(K5)=Z(K5)+U8-U9
      Z(K6)=U8+U9
      IF(IP.EQ.1) GO TO 24
      Z(K1)=Z(K1)+U5+U7
      Z(K3)=Z(K3)+U6-U7
      Z(K7)=Z(K7)+UC-UD
      IF(IP.EQ.MP) GO TO 22
   24 Z(K2)=Z(K2)+U5-U7
      Z(K4)=U6+U7
      Z(K8)=UC+UD
   22 Z(K8+MT)=U2*(D8*(H5A+D4*H5B)-A1*UD)
      JM=JM+N2
   31 CONTINUE
   16 CONTINUE
      JN=JN+N
   15 CONTINUE
      DO 100 LSS=1,N
      LS=LSS-1
      Z(LS*N+NP1)=(0.,0.)
      Z(LS*N+NP1-1)=(0.,0.)
  100 Z(LS*N+NP1+MT)=(0.,0.)
      DO 101 LS=1,N
      Z((NP1-2)*N+LS)=(0.,0.)
      Z((NP1-1)*N+LS)=(0.,0.)
  101 Z((NP1-1+MT)*N+LS)=(0.,0.)
      Z((NP1-2)*N+NP1-1)=(1.,0.)
      Z((NP1-1)*N+NP1)=(1.,0.)
      Z((MT+NP1-1)*N+NP1+MT)=(1.,0.)
      RETURN
      END
      SUBROUTINE SPHERE(FEXP,FHXP,NP1,NP2,NT,RH,ZH,XT,AT,BK,R)
C
C     SPHERICAL WAVE EXCITATION VECTOR - SOURCE ON Z AXIS
C    (r=+1,-1 ONLY). DISTANCE BETWEEN ORIGINS (O TO O') IS ZF
C
      COMPLEX R(2000),U,U2,U3,CEXP,PSI(300),F1E,F2E,F3E,F4E,
      COMPLEX CMPLX,U0,UES,UEC,UH,F1H,F2H
      DIMENSION TH(10),RH(300),ZH(300),XT(10),AT(10)
      NP=NP1+NP2
      MP=NP-1
      MT=MP-1
      N=MT+MP
      U=(0.,1.)
      PI=3.141593
      PI2=PI/2.
      DO 12 IP=1,MP
      K2=IP
      I=IP+1
      DR=.5*(RH(I)-RH(IP))
      DZ=.5*(ZH(I)-ZH(IP))
```

```
      D1=SQRT(DR*DR+DZ*DZ)
      R1=.5*(RH(I)+RH(IP))
      IF(ABS(R1).LT.1.E-5) R1=1.
      Z1=.5*(ZH(I)+ZH(IP))
      SVP=DR/D1
      CVP=DZ/D1
      DO 13 L=1,NT
      QS=DR*XT(L)
      QC=DZ*XT(L)
      TH(L)=ATAN2((R1+QS),(Z1+QC))
      RP=SQRT((R1+QS)**2+(Z1+QC)**2)
      PSI(L)=CEXP(CMPLX(0.,-RP))/RP
   13 CONTINUE
      F1E=(0.,0.)
      F2E=(0.,0.)
      F3E=(0.,0.)
      F4E=(0.,0.)
      F1H=(0.,0.)
      F2H=(0.,0.)
      DO 15 L=1,NT
      U0=AT(L)*PSI(L)
      UES=FE(FEXP,TH(L))*SIN(TH(L))*U0
      UEC=FE(FEXP,TH(L))*COS(TH(L))*UC
      UH=U0*FH(FHXP,TH(L))
      F1E=F1E+UES
      F2E=F2E+UEC
      F3E=F3E+UES*XT(L)
      F4E=F4E+UEC*XT(L)
      F1H=F1H+UH
      F2H=F2H+UH*XT(L)
   15 CONTINUE
      U2=-D1*PI2*(CVP*F1E-SVP*F2E)
      U3=-D1*PI2*(CVP*F3E-SVP*F4E)
      K1=K2-1
      R(K2+MT)=D1*U*PI*(F1H+D1*SVP*F2H/R1)
      IF(IP.EQ.1) GO TO 21
      R(K1)=R(K1)+U2-U3
      IF(IP.EQ.MP) GO TO 27
   21 R(K2)=U2+U3
   27 CONTINUE
   12 CONTINUE
C
C SIMPLIFIED METHOD FOR HANDLING MULTIPLE BODIES
C
      R(NP1-1)=(0.,0.)
      R(NP1)=(0.,0.)
      R(NP1+MT)=(0.,0.)
      RETURN
      END
      SUBROUTINE SOLVE(N,IPS,UL,B,X)
      COMPLEX UL(300000),B(500),X(500),SUM
```

```
 1          DIMENSION IPS(500)
 2          NP1=N+1
 3          IP=IPS(1)
 4          X(1)=B(IP)
 5          DO 2 I=2,N
 6          IP=IPS(I)
 7          IPB=IP
 8          IM1=I-1
 9          SUM=(0.,0.)
10          DO 1 J=1,IM1
11          SUM=SUM+UL(IP)*X(J)
12        1 IP=IP+N
13        2 X(I)=B(IPB)-SUM
14          K2=N*(N-1)
15          IP=IPS(N)+K2
16          X(N)=X(N)/UL(IP)
17          DO 4 IBACK=2,N
18          I=NP1-IBACK
19          K2=K2-N
20          IPI=IPS(I)+K2
21          IP1=I+1
22          SUM=(0.,0.)
23          IP=IPI
24          DO 3 J=IP1,N
25          IP=IP+N
26        3 SUM=SUM+UL(IP)*X(J)
27        4 X(I)=(X(I)-SUM)/UL(IPI)
28          RETURN
29          END
30          SUBROUTINE DECOMP(N,IPS,UL)
31          COMPLEX UL(300000),PIVOT,EM
32          DIMENSION SCL(500),IPS(500)
33          DO 5 I=1,N
34          IPS(I)=I
35          RN=0.
36          J1=I
37          DO 2 J=1,N
38          ULM=ABS(REAL(UL(J1)))+ABS(AIMAG(UL(J1)))
39          J1=J1+N
40          IF(RN-ULM) 1,2,2
41        1 RN=ULM
42        2 CONTINUE
43          SCL(I)=1./RN
44        5 CONTINUE
45          NM1=N-1
46          K2=0
47          DO 17 K=1,NM1
48          BIG=0.
49          DO 11 I=K,N
50          IP=IPS(I)
51          IPK=IP+K2
```

```
      SIZE=(ABS(REAL(UL(IPK)))+ABS(AIMAG(UL(IPK))))*SCL(IP)
      IF(SIZE-BIG) 11,11,10
   10 BIG=SIZE
      IPV=I
   11 CONTINUE
      IF(IPV-K) 14,15,14
   14 J=IPS(K)
      IPS(K)=IPS(IPV)
      IPS(IPV)=J
   15 KPP=IPS(K)+K2
      PIVOT=UL(KPP)
      KP1=K+1
      DO 16 I=KP1,N
      KP=KPP
      IP=IPS(I)+K2
      EM=-UL(IP)/PIVOT
   18 UL(IP)=-EM
      DO 16 J=KP1,N
      IP=IP+N
      KP=KP+N
      UL(IP)=UL(IP)+EM*UL(KP)
   16 CONTINUE
      K2=K2+N
   17 CONTINUE
      RETURN
      END
      FUNCTION BLOG(X)
      IF(X.GT..1) GO TO 1
      X2=X*X
      BLOG=((.075*X2-.1666667)*X2+1.)*X
      RETURN
    1 BLOG=ALOG(X+SQRT(1.+X*X))
      RETURN
      END
      FUNCTION FE(FEXP,X)
      PI2=3.14159/2.
      FE=0.
      IF(ABS(X).LE.PI2) FE=ABS(COS(X))**FEXP
      RETURN
      END
      FUNCTION FH(FHXP,X)
      PI2=3.14159/2.
      FH=0.
      IF(ABS(X).LE.PI2) FH=-ABS(COS(X))**FHXP
      RETURN
      END
      SUBROUTINE PLANE(M1,M2,NP1,NP2,NT,RH,ZH,XT,AT,THR,R)
C
C Unchanged version from Mautz and Harrington report.
C
      COMPLEX R(2000),U,U1,UA,UB,FA(10),FB(10),F2A,F2B,F1A,F1B
```

```
      COMPLEX U2,U3,U4,U5,cmplx
      DIMENSION RH(300),ZH(300),XT(10),AT(10),R2(10),Z2(10)
      DIMENSION BJ(5000)
      NP=NP1+NP2
      MP=NP-1
      MT=MP-1
      N=MT+MP
      N2=2*N
      CC=COS(THR)
      SS=SIN(THR)
   11 CONTINUE
      U=(0.,1.)
      U1=3.141593*U**M1
      M3=M1+1
      M4=M2+3
      IF(M1.EQ.0) M3=2
      M5=M1+2
      M6=M2+2
      DO 12 IP=1,MP
      K2=IP
      I=IP+1
      DR=.5*(RH(I)-RH(IP))
      DZ=.5*(ZH(I)-ZH(IP))
      D1=SQRT(DR*DR+DZ*DZ)
      R1=.25*(RH(I)+RH(IP))
      IF(R1.EQ.0.) R1=1.
      Z1=.5*(ZH(I)+ZH(IP))
      DR=.5*DR
      D2=DR/R1
      DO 13 L=1,NT
      R2(L)=R1+DR*XT(L)
      Z2(L)=Z1+DZ*XT(L)
   13 CONTINUE
      D3=DR*CC
      D4=-DZ*SS
      D5=D1*CC
      DO 23 M=M3,M4
      FA(M)=0.
      FB(M)=0.
   23 CONTINUE
      DO 15 L=1,NT
      X=SS*R2(L)
      IF(X.GT..5E-7) GO TO 19
      DO 20 M=M3,M4
      BJ(M)=0.
   20 CONTINUE
      BJ(2)=1.
      S=1.
      GO TO 18
   19 M=2.8*X+14.-2./X
      IF(X.LT..5) M=11.8+ALOG10(X)
```

```
      IF(M.LT.M4) M=M4
      BJ(M)=0.
      JM=M-1
      BJ(JM)=1.
      DO 16 J=4,M
      J2=JM
      JM=JM-1
      J1=JM-1
      BJ(JM)=J1/X*BJ(J2)-BJ(JM+2)
   16 CONTINUE
      S=0.
      IF(M.LE.4) GO TO 24
      DO 17 J=4,M,2
      S=S+BJ(J)
   17 CONTINUE
   24 S=BJ(2)+2.*S
   18 ARG=Z2(L)*CC
      UA=AT(L)/S*CMPLX(COS(ARG),SIN(ARG))
      UB=XT(L)*UA
      DO 25 M=M3,M4
      FA(M)=BJ(M)*UA+FA(M)
      FB(M)=BJ(M)*UB+FB(M)
   25 CONTINUE
   15 CONTINUE
      IF(M1.NE.0) GO TO 26
      FA(1)=FA(3)
      FB(1)=FB(3)
   26 UA=U1
      DO 27 M=M5,M6
      M7=M-1
      M8=M+1
      F2A=UA*(FA(M8)+FA(M7))
      F2B=UA*(FB(M8)+FB(M7))
      UB=U*UA
      F1A=UB*(FA(M8)-FA(M7))
      F1B=UB*(FB(M8)-FB(M7))
      U4=D4*UA
      U2=D3*F1A+U4*FA(M)
      U3=D3*F1B+U4*FB(M)
      U4=DR*F2A
      U5=DR*F2B
      K1=K2-1
      K4=K1+N
      K5=K2+N
      R(K2+MT)=-D5*(F2A+D2*F2B)
      R(K5+MT)=D1*(F1A+D2*F1B)
      IF(IP.EQ.1) GO TO 21
      R(K1)=R(K1)+U2-U3
      R(K4)=R(K4)+U4-U5
      IF(IP.EQ.MP) GO TO 22
   21 R(K2)=U2+U3
```

```
      R(K5)=U4+U5
   22 K2=K2+N2
      UA=UB
   27 CONTINUE
   12 CONTINUE
      R(NP1-1)=(0.,0.)
      R(NP1)=(0.,0.)
      R(NP1+MT)=(0.,0.)
      RETURN
      END
      SUBROUTINE PLAN(M1,M2,NP,NT,RH,ZH,XT,AT,THR,R)
C
C PLANE WAVE RECEIVE VECTOR ELEMENTS. CAN BE USED TO COMPUTE
C THE PLANE WAVE EXCITATION ELEMENTS IF PLANE WAVE SCATTERING
C IS BEING CALCULATED. (THE RELATIONSHIP BETWEEN THE RECEIVE
C AND  EXCITAION ELEMENTS AS DISCUSSED BY MAUTZ AND
C HARRINGTON.)
C
      COMPLEX R(1800),U,U1,UA,UB,FA(5),FB(5),F2A,F2B,F1A,F1B
      COMPLEX U2,U3,U4,U5,CMPLX
      DIMENSION RH(1000),ZH(1000),XT(10),AT(10),R2(10)
      DIMENSION Z2(10),BJ(5000)
      MP=NP-1
      MT=MP-1
      N=MT+MP
      N2=2*N
      CC=COS(THR)
      SS=SIN(THR)
      U=(0.,1.)
      U1=3.141593*U**M1
      M3=M1+1
      M4=M2+3
      IF(M1.EQ.0) M3=2
      M5=M1+2
      M6=M2+2
      DO 12 IP=1,MP
      K2=IP
      I=IP+1
      DR=.5*(RH(I)-RH(IP))
      DZ=.5*(ZH(I)-ZH(IP))
      D1=SQRT(DR*DR+DZ*DZ)
      R1=.25*(RH(I)+RH(IP))
      IF(R1.EQ.0.) R1=1.
      Z1=.5*(ZH(I)+ZH(IP))
      DR=.5*DR
      D2=DR/R1
      DO 13 L=1,NT
      R2(L)=R1+DR*XT(L)
      Z2(L)=Z1+DZ*XT(L)
   13 CONTINUE
      D3=DR*CC
```

```
      D4=-DZ*SS
      D5=D1*CC
      DO 23 M=M3,M4
      FA(M)=0.
      FB(M)=0.
   23 CONTINUE
      DO 15 L=1,NT
      X=SS*R2(L)
      IF(X.GT..5E-7) GO TO 19
      DO 20 M=M3,M4
      BJ(M)=0.
   20 CONTINUE
      BJ(2)=1.
      S=1.
      GO TO 18
   19 M=2.8*X+14.-2./X
      IF(X.LT..5) M=11.8+ALOG10(X)
      IF(M.LT.M4) M=M4
      BJ(M)=0.
      JM=M-1
      BJ(JM)=1.
      DO 16 J=4,M
      J2=JM
      JM=JM-1
      J1=JM-1
      BJ(JM)=J1/X*BJ(J2)-BJ(JM+2)
   16 CONTINUE
      S=0.
      IF(M.LE.4) GO TO 24
      DO 17 J=4,M,2
      S=S+BJ(J)
   17 CONTINUE
   24 S=BJ(2)+2.*S
   18 ARG=Z2(L)*CC
      UA=AT(L)/S*CMPLX(COS(ARG),SIN(ARG))
      UB=XT(L)*UA
      DO 25 M=M3,M4
      FA(M)=BJ(M)*UA+FA(M)
      FB(M)=BJ(M)*UB+FB(M)
   25 CONTINUE
   15 CONTINUE
      IF(M1.NE.0) GO TO 26
      FA(1)=FA(3)
      FB(1)=FB(3)
   26 UA=U1
      DO 27 M=M5,M6
      M7=M-1
      M8=M+1
      F2A=UA*(FA(M8)+FA(M7))
      F2B=UA*(FB(M8)+FB(M7))
      UB=U*UA
```

```
 1          F1A=UB*(FA(M8)-FA(M7))
 2          F1B=UB*(FB(M8)-FB(M7))
 3          U4=D4*UA
 4          U2=D3*F1A+U4*FA(M)
 5          U3=D3*F1B+U4*FB(M)
 6          U4=DR*F2A
 7          U5=DR*F2B
 8          K1=K2-1
 9          K4=K1+N
10          K5=K2+N
11          R(K2+MT)=-D5*(F2A+D2*F2B)
12          R(K5+MT)=D1*(F1A+D2*F1B)
13          IF(IP.EQ.1) GO TO 21
14          R(K1)=R(K1)+U2-U3
15          R(K4)=R(K4)+U4-U5
16          IF(IP.EQ.MP) GO TO 22
17       21 R(K2)=U2+U3
18          R(K5)=U4+U5
19       22 K2=K2+N2
20          UA=UB
21       27 CONTINUE
22       12 CONTINUE
23          RETURN
24          END
25
```

LIST OF REFERENCES

1. Collin, R. E., Antennas And Radiowave Propagation, pp. 253-259, McGraw-Hill, 1985.

2. Skolnik, M. I., Radar Handbook, pp. 6.23-6.25, McGraw-Hill, 1990.

3. Hannan, P. W., Microwave Antennas Derived from the Cassegrian Telescope, IRE Trans. Antennas Propagat., Vol. Ap-9, pp. 140-153, March 1961.

4. Balanis, C. A., Antenna Theory Analysis and Design, pp. 637-642, John Wiley & Sons, Inc., 1982.

5. Yerukhhimovich, Y. A., "Analaysis of Two-Mirror Antennas of a General Type", Telecom. and Radio Engineering, Part 2, 27, No. 11, pp. 97-103, 1972.

6. Rotman, W., and Lee, J. C., "Compact Dual-Frequency Reflector Antennas for EHF Mobile Satellite Communication Terminals," IEEE AP-S International Symposium Digest, II, Boston, Massachusetts, pp. 771-774, June 1984.

7. Balanis, C. A., Advanced Engineering Electromagnetic, pp. 670-712, John Wiley & Sons, Inc., 1989.

8. Harrington, R. F., and Mautz, J. R., "Radiation And Scattering From Bodies Of Revolution, Final Rep., AFCRL-69-0305, Syracuse Univ., Syracuse, NY, July 1969.

9. Harrington, R. F., and Mautz, J. R., "H-FIELD, E-FIELD, AND COMBINED FIELD SOLUTION FOR BODIES OF REVOLUTION", TECHNICAL REPORT TR-77-2, SYracuse Univ., Syracuse, N.Y., February 1977.

10. Harrington, R. F., and Mautz, J. R., " AN IMPROVED E-FIELD SOLUTION FOR A CONDUCTIVE BODY OF REVOLUTION ", TECHNICAL REPORT TR-80-1, Syracuse Univ., Syracuse, N.Y., 1980.

INITIAL DISTRIBUTION LIST

1.	Library, Code 52 Naval Postgraduate School Monterey, CA 93943-5002	2
2.	Chairman, Code EC Department of Electrical and Computer Engineering Naval Postgraduate School Monterey, CA 93943-5002	1
3.	Professor D. C. Jenn, Code EC/Jn Department of Electrical and Computer Engineering Naval Postgraduate School Monterey, CA 93943-5002	1
4.	Professor H. M. Lee, Code EC/Lh Department of Electrical and Computer Engineering Naval Postgraduate School Monterey, CA 93943-5002	1
5.	Aluizio Prata, Assistant Professor Department of Electrical Engineering University of Southern California Los Angeles, CA 90089-0271	1
6.	Defense Technical Information Center Cameron Station Alexandria, VA 22304-6145	2
7.	Naval Attache Embassy of Israel 3514 International Drive, N.W. Washington, D.C. 20008	1
8.	The Head Of Electrical Division, Israeli Navy Via Naval Attache Embassy of Israel 3514 International Drive, N.W. Washington, D.C. 20008	1
9.	Vered Nissan Louis Marshal 7 Street Tel-Aviv, Zip Code: 62668 Israel	2